# NAVAL POSTGRADUATE SCHOOL
## Monterey, California


# THESIS

ACOUSTIC TRANSIENT TDOA ESTIMATION AND DISCRIMINATION

by

Granger Hart Bennett

September 2000

Thesis Advisors: Charles W. Therrien
Murali Tummala
Kevin B. Smith

**Approved for public release; distribution is unlimited**

# REPORT DOCUMENTATION PAGE

Form Approved
OMB No. 0704-0188



| 1. AGENCY USE ONLY *(Leave blank)* | 2. REPORT DATE<br>September 2000 | 3. REPORT TYPE AND DATES COVERED<br>Master's Thesis |
|---|---|---|

| 4. TITLE AND SUBTITLE: Acoustic Transient TDOA Estimation and Discrimination | 5. FUNDING NUMBERS |
|---|---|
| 6. AUTHOR(S) Bennett, Granger Hart | |
| 7. PERFORMING ORGANIZATION NAME(S) AND ADDRESS(ES)<br>Naval Postgraduate School<br>Monterey, CA 93943-5000 | 8. PERFORMING ORGANIZATION REPORT NUMBER |
| 9. SPONSORING / MONITORING AGENCY NAME(S) AND ADDRESS(ES)<br>Assault and Special Mission Programs PMA-264<br>47123 Buse RD IPT Ste 148<br>Patuxent River, MD 20670-1547 | 10. SPONSORING / MONITORING AGENCY REPORT NUMBER |

**11. SUPPLEMENTARY NOTES**
The views expressed in this thesis are those of the author and do not reflect the official policy or position of the Department of Defense or the U.S. Government.

| 12a. DISTRIBUTION / AVAILABILITY STATEMENT<br>Approved for public release; distribution is unlimited | 12b. DISTRIBUTION CODE |
|---|---|

**13. ABSTRACT** *(Maximum 200 words)*

This thesis examines acoustic transient discrimination and Time Difference Of Arrival (TDOA) estimation for the purposes of estimating the position of a submarine in a sonabuoy field. Transient discrimination, for this thesis, is the process of telling different transients apart. Two algorithms are evaluated. One method is based on higher order statistics while the other is based on signal subspace techniques. Extensive simulations using synthetic transients were conducted to establish the performance of each algorithm in terms of discrimination and TDOA estimation. It was found that the bispectral algorithm gave better TDOA estimation at low SNRs while the subspace algorithm gave better TDOA estimation at high SNRs. For discrimination, it was found that the subspace algorithm gave consistant false alarm rates at all SNRs while the false alarm rate for the bispectral algorithm grew with increasing SNR.

| 14. SUBJECT TERMS<br>Transient, TDOA, Discrimination, bispectrum, subspace | 15. NUMBER OF PAGES<br>80 |
|---|---|
| | 16. PRICE CODE |

| 17. SECURITY CLASSIFICATION OF REPORT<br>Unclassified | 18. SECURITY CLASSIFICATION OF THIS PAGE<br>Unclassified | 19. SECURITY CLASSIFICATION OF ABSTRACT<br>Unclassified | 20. LIMITATION OF ABSTRACT |
|---|---|---|---|

NSN 7540-01-280-5500

Standard Form 298 (Rev.2-89)
Prescribed by ANSI Std. 239-18

**Approved for public release; distribution is unlimited**

# ACOUSTIC TRANSIENT TDOA ESTIMATION AND DISCRIMINATION

Granger Hart Bennett
Lieutenant Commander, South African Navy
B.Eng, University of Stellenbosch South Africa, 1991

Submitted in partial fulfillment of the
requirements for the degrees of

**MASTER OF SCIENCE IN ELECTRICAL ENGINEERING**
**MASTER OF SCIENCE IN ENGINEERING ACOUSTICS**

from the

**NAVAL POSTGRADUATE SCHOOL**

**September 2000**

## ABSTRACT

This thesis examines acoustic transient discrimination and Time Difference Of Arrival (TDOA) estimation for the purposes of estimating the position of a submarine in a sonabuoy field. Transient discrimination, for this thesis, is the process of telling different transients apart. Two algorithms are evaluated. One method is based on higher order statistics while the other is based on signal subspace techniques. Extensive simulations using synthetic transients were conducted to establish the performance of each algorithm in terms of discrimination and TDOA estimation. It was found that the bispectral algorithm gave better TDOA estimation at low SNRs while the subspace algorithm gave better TDOA estimation at high SNRs. For discrimination, it was found that the subspace algorithm gave consistant false alarm rates at all SNRs while the false alarm rate for the bispectral algorithm grew with increasing SNR.

## TABLE OF CONTENTS

## LIST OF FIGURES

## LIST OF TABLES

## ACRONYMS AND ABBREVIATIONS

| | |
|---|---|
| TDOA | Time Difference Of Arrival |
| ASW | Anti-Submarine Warfare |
| Gram | Sonogram |
| SPL | Sound Pressure Level |
| SIGINT | SIGnal INTelligence |
| PSD | Power Spectral Density |
| AR | Autoregression |
| MA | Moving Average |
| ARMA | Autoregressive Moving Average |
| MUSIC | Multiple Signal Classification |
| PCLP | Principle Components Linear Prediction |
| PHAT | Phase Transform |
| LFM | Linear Phase Modulated |
| CW | Continuous Wave |
| SNR | Signal-to-Noise Ratio |

## EXECUTIVE SUMMARY

In this thesis we have developed and compared two algorithms, namely the bispectrum and subspace linear phase detectors. These algorithms were developed for the purposes of transient discrimination and Time-Difference-Of-Arrival (TDOA) estimation. They are to be used as part of a transient tool suite to aid in the estimation of a submarine's position. Two performance measures were used to evaluate the algorithms, namely the probability of correct TDOA ($P_T$) and the probability of correct discrimination ($P_{Di}$).

In general, it can be said that for TDOA, the bispectral linear phase detector gave better results at low SNRs while the subspace linear phase detector worked better at the higher SNRs.

For discrimination, it was found that the bispectral discriminator gave higher $P_{Di}$ than the subspace discriminator. However, the probability of false discrimination ($P_{fa}$) of the bispectral discriminator increased at higher SNRs while the subspace discriminator gave a constant $P_{fa}$ for all SNRs evaluated. For discrimination, the advantage of having a constant $P_{fa}$ is desirable. Therefore the subspace discriminator is the best option even although it produced lower $P_{Di}$ than the bispectral discriminator. It was also found that there are design trade-offs between processing speed and performance that need to be made. For the bispectral linear phase detector, this trade-off is in terms of threshold gain; for the subspace linear phase detector, this trade-off is in terms of correlation matrix size.

## ACKNOWLEDGEMENTS

I would like to thank my thesis advisors, Professors Charles Therrien, Murrali Tummala and Kevin Smith for all their advice, guidance and availability during this thesis.

Furthermore I would like to thank my wife, Minette, for all her patience, encouragement and support during my studies and for this thesis.

# I. INTRODUCTION

The work of this thesis forms part of the ongoing effort to automate the detection, discrimination and Time-Difference-Of-Arrival (TDOA) estimation of transient signals. At present, transient signals are located and processed manually, making it a very time consuming procedure. It is therefore more desirable to have an automated system that can deliver the same or better results than the present manual approach.

For this thesis, it is assumed that the detection of the transient has already taken place; therefore, the objective of the thesis is to look at discrimination and TDOA estimation only. Two algorithms, namely the bispectral linear phase detector and the subspace linear phase detector, are developed for this purpose.

## A. THE OPERATIONAL MISSION

A typical mission considered for this thesis starts off with an anti-submarine warfare (ASW) aircraft laying a sonabuoy field in the vicinity or on the predicted path of a submarine. Usually each sonabuoy in the field consists of calibrated omni-directional passive acoustic sensors. The ASW aircraft collects acoustic data on a target submarine as it passes through the sonabuoy field.

Figure 1 shows a typical V-shaped sonabuoy field that can be used in this type of mission. When this shape is used, the target must pass through the apex of the V of the field (as close as possible) in order to obtain the most accurate results. The data received at the sonabuoys is transmitted to the aircraft, which in turn records the data on tape for mission post processing.

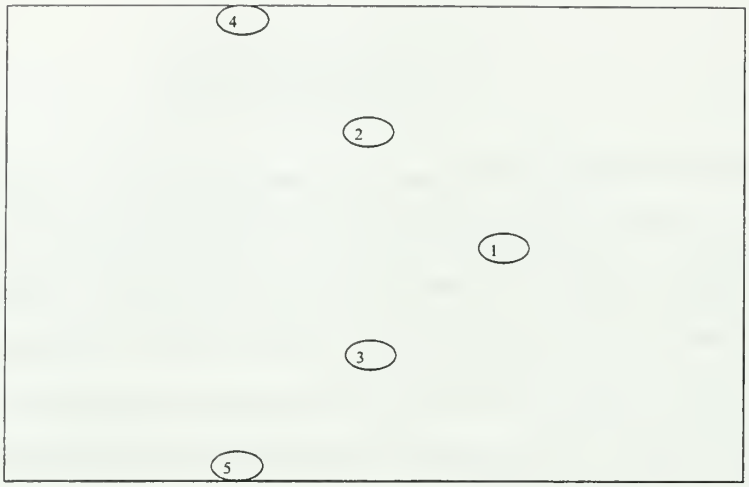


**Figure 1. Typical Sonabuoy Field.**

The data collected on the tapes is processed at an onshore location in order to estimate the acoustic Sound Pressure Levels (SPL) of tonals, broadband signals and transients that are emitted from the submarine.

To obtain precise SPL of a submarine, an accurate track is required so that the pressure levels received at the sonabuoys can be projected back to estimate the pressure levels at the target. For best results, the position of each sonabuoy must be known, the target must be on a course that passes through the middle of the field, and an accurate estimation of TDOA of acoustic signals must be made.

## B. DATA PROCESSING

The data collected from the sonabuoys and stored on the tape is processed by first generating a baseband sonogram. A sonogram is a frequency versus time plot of the acoustic pressure levels at a sonabuoy. From these sonograms an analyst can identify and highlight contact events of interest, which may include signals, such as narrowband tonals and transients. The events identified are then processed to obtain an estimate of the target's track. Once the best estimate of the target track has been made, the analyst can conduct SPL analysis on all types of previously identified contact signals. The final desired results are the SPL signature characteristics for a given target with respect to aspect angle.

At present, transient analysis is a manually intensive operation. Typically, the analyst marks transient events of interest from the sonogram display of a sonabuoy and then searches the sonograms of the other sonabuoys for the same transient. This can be a very time consuming process since in a single mission there can be hundreds of transients within a single sonogram. These must be matched up to those on the sonograms from the other sonabuoys in the sonabuoy field.

## C. THESIS GOAL

The goal of this thesis is to develop and evaluate two algorithms that can be used for transient discrimination and Time-Difference-Of-Arrival (TDOA) estimation. The two algorithms are the bispectral linear phase detector and the subspace linear phase detector.

## D. THESIS OUTLINE

The remainder of this thesis is organized as follows. Chapter II discusses transients and transient processing and introduces the problems of interest, namely TDOA estimation and transient discrimination. Chapter III presents the relevant signal models and the analysis of the measured signals in terms of second- and third-order moments. This chapter details the formulation of the bispectral linear phase detector and discriminator. Chapter IV discusses signal subspace techniques and their application to the problem of TDOA estimation and transient discrimination. The outcome of this chapter is the formulation of the subspace TDOA estimator and discriminator. Chapter V examines the results achieved by both the bispectral and subspace TDOA estimators and discriminators. Extensive simulations are conducted using synthetic transients to produce performance curves and to study the utility of each technique in discrimination and TDOA of transients. Chapter VI provides conclusions and recommendations for future work based on the results presented. Appendix A and Appendix B show the discrimination results for the different combinations of signals not shown in Chapter V.

THIS PAGE INTENTIONALLY LEFT BLANK

# II. TRANSIENT PROCESSING

## A. TRANSIENT SIGNALS

Transients of interest here are short duration wideband acoustic signals. Accordingly transients can be of varying shapes and lengths, lasting anywhere from a few microseconds to a couple of seconds. Typical examples of these signals are a wrench falling on a metal deck or the sounds of a biological life form, such as a whale. Due to the diversity of these signals, there is limited *a priori* information that can be used to aid in their detection. When transients are imbedded in noise, their detection becomes very difficult because the energy in the noise frequently dominates the energy in the transient over the interval of interest. Nevertheless, in conjunction with other measurements or by themselves, transients can be used to estimate the track of the target submarine by estimating the TDOA of a transient between two sonabuoys.

Tracking of a submarine using transients requires transient detection, discrimination and TDOA estimation. Prior to discrimination, a transient must be *detected* in a noisy background on the sonagram of a single sonabuoy. This thesis does not address the transient detection problem and therefore assumes that a transient has been detected on the sonogram of a sonabuoy.

After the transient has been detected, the same transient must be found on the sonograms of the other sonabuoys in the sonabuoy field. This is difficult since the detected transient may not exist on all sonabuoys within the field. That is, the sonograms of the other sonabuoys could contain only noise or even a different transient in the window of interest. The first case (i.e., where the sonogram of the other sonabuoys contain only noise) is a common scenario. This happens because transients can be very localized and thus do not appear on the sonograms of each sonabuoy. The second case (i.e., where a different transient exists on the sonogram of the second sonabuoy) is also common due to the complex environment of the mission, where multiple transients from different sources can exist on the data records of the other sonabuoys in the field. It is therefore important to *discriminate* between different transients and to know if there is no transient present. If the transients arriving at two or more different sonabuoys are the

same, then TDOA estimates can be used for target localization. In the following we first discuss TDOA estimation and then transient discrimination.

## B. TIME DIFFERENCE OF ARRIVAL (TDOA) ESTIMATION

TDOA estimation is by no means simple and therefore many authors have written about it [Ref 1]. It is, however, the primary means of determining range to the target in passive detection, since TDOA information from multiple sonabuoys and the geometry of the sonabuoy field can be used to determine the position of the submarine at any particular instance in time. For any given value of TDOA between two sonabuoys, the locus of possible target positions is a hyperbolic curve. If more than one curve can be drawn, i.e., if TDOA values between three or more sonabuoys can be calculated, the intersection of the curves determines the position of the target.

Consider a simple two-buoy model as shown in Figure 2. The sonabuoys are symmetrically positioned about the origin on the x-axis as shown in Figure 2, with the target located at T.

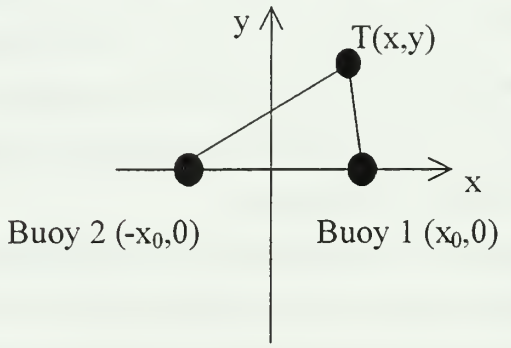


**Figure 2. Two Symmetrically Positioned Sonabuoys.**

For this geometry the time delay $\tau$ between sonabuoy 1 and sonabuoy 2 is given by

$$\tau = t_1 - t_2 = \frac{D_{t_1}}{c} - \frac{D_{t_2}}{c}$$
$$(\tau \cdot c)^2 = (\sqrt{(x_0 - x)^2 + y^2} - \sqrt{(x_0 + x)^2 + y^2})^2 \qquad (2.1)$$

where $c$ is the speed of sound, $D_{t_1}$ and $D_{t_2}$ are the distances between the target and sonabuoy 1 and sonabuoy 2, respectively. After some algebraic manipulation[1] of Eq. 2.1, the following expression is obtained [Ref 1]:

$$\frac{x^2}{a^2} - \frac{y2}{b^2} = 1 \qquad (2.2)$$

where

$$a = \frac{\tau . c}{2}$$

$$b = \sqrt{\left(\frac{2x_0}{2}\right)^2 - a^2}$$

Equation 2.2 describes a hyperbola, and a set of hyperbolas can be drawn for different TDOA's between sonabuoy 1 and 2 as shown in Figure 3.

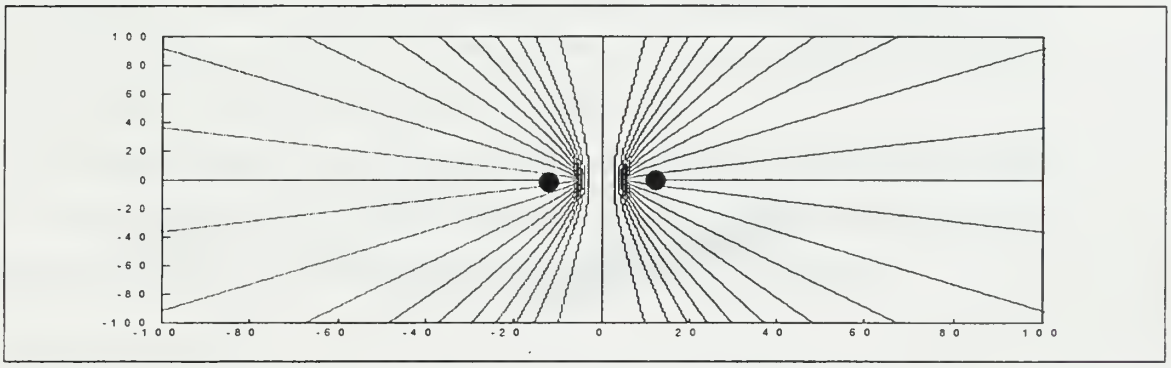


**Figure 3. Hyperbolic curves for TDOA between two symmetrically positioned sonabuoys. Sonabuoy positions are indicated by the dots.**

## C. TRANSIENT DISCRIMINATION

The objective of discrimination between transients is to be able to tell different transients apart. This is different from transient classification or transient characterization, which attempts to identify the source of the transient and seeks to group similar transients together.

[1] To obtain a hyperbolic expression, Eq 2.1 must be squared, and all the cross terms must be left on the right hand side and all other terms on the left hand side. Both sides must now be squared again with like terms collected.

Discrimination is difficult since it relies on detecting differences between the two received signals. These differences can be either in magnitude or phase or both. The problem is further complicated by the presence of noise and the fact that (due to differences in propagation path characteristics) the same transient arriving at two different locations may not look and sound the same. Achieving good discrimination at low SNR values is a challenging task.

Figure 4 shows some typical cases in which transient discrimination has to take place. The cases shown in this figure are a *localized* transient such as an expanding bubble on a sonabuoy, a directional transient that is emitted from the hull of the submarine and is only received at some of the sonabuoys in the sonabuoy field, and an omnidirectional transient that is received at all sonabuoys in the field.

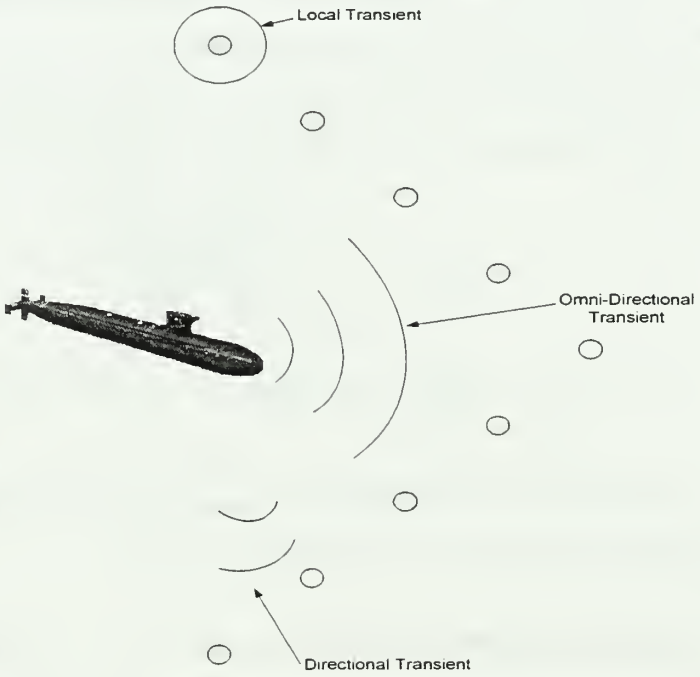


**Figure 4. Discrimination Cases.**

Considering these cases, the TDOA cannot be estimated for all combinations of two sonabuoys in the field. Further, if a transient arriving at one sonabuoy is mistaken to be the same as the transient arriving at another sonabuoy, the resulting TDOA estimate will produce an erroneous target position. This in turn may lead to errors in tracking and ultimately possible erroneous SPL calculations.

# III. MOMENT-BASED SIGNAL PROCESSING

Most of the traditional work on transient processing and TDOA estimation is based on the use of second order statistics and classical (i.e., Fourier-based) methods of spectrum estimation [Ref 2], [Ref 3], [Ref 4], [Ref 5], [Ref 6]. Recently, new work has appeared using techniques involving higher order moments of signals and higher order spectra, such as the bispectrum [Ref 7].

The motivation for using the bispectrum in transient discrimination and TDOA estimation is twofold. First, the higher order spectra suppress Gaussian noise processes of unknown spectral characteristics. Secondly, these spectra, unlike the usual power density spectrum, preserve phase information [Ref 7]. In the last few years there has been a considerable amount of new research done in using the bispectrum and trispectrum for transient detection, time delay estimation and classification of signals [Ref 7:p 313], [Ref 8], [Ref 9], [Ref 10], [Ref 11], [Ref 12].

This chapter defines the signal model used in this thesis and the analysis of these signals based on second and third moments. Finally, a set of algorithms for discrimination and TDOA estimation using third order moments is discussed.

## A. SIGNAL MODEL

Before any further analysis can be done it is necessary to develop a signal model, which can be used for the analysis of transients arriving at two sonabuoys. As mentioned previously, there are three cases to be considered. In the first case, the transient arriving at the second sonabuoy is the same as the transient arriving at the first sonabuoy. In the second case, the two arriving transient signals are different while in the third case only noise is present at the second sonabuoy. It is also assumed that the sonabuoys used are omni-directional and that their separation in the sonabuoy field is large enough so that noise at the first sonabuoy is uncorrelated with noise at the second sonabuoy in both space and time.

The following simple model can be used to represent a single transient arriving at two different sonabuoys:

$$x_1(k) = s(k) + \eta_1(k)$$
$$x_2(k) = As(k-L) + \eta_2(k), \tag{3. 1}$$

where $x_i(k)$ is the noise-embedded signal arriving at sonabuoy $i$, $s(k)$ is the transient signal itself, and $\eta_i(k)$ is white gaussian noise. Note that the signal at sonabuoy 2 is subject to a relative attenuation $A$ and delay $L$ with respect to the signal at sonabuoy 1. The frequency domain expression for these signals is

$$X_1(\omega) = S(\omega) + N_1(\omega)$$
$$X_2(\omega) = S(\omega)e^{-j\omega L} + N_2(\omega), \tag{3. 2}$$

where the uppercase letters represent Fourier transforms of the respective signals in Eq. 3.1.

If the transient arriving at sonabuoy 2 is different from the transient arriving at sonabuoy 1, the received signals are given by:

$$x_1(k) = s(k) + \eta_1(k)$$
$$x_2(k) = r(k-L) + \eta_2(k), \tag{3. 3}$$

where $r(k)$ is the other transient arriving at sonabuoy 2 with time delay $L$ relative to $s(k)$. The corresponding expressions in the frequency domain are

$$X_1(\omega) = S(\omega) + N_1(\omega)$$
$$X_2(\omega) = R(\omega)e^{-j\omega L} + N_2(\omega). \tag{3. 4}$$

If there is no transient present at the second sonabuoy, the two received signals are

$$x_1(k) = s(k) + n_1(k)$$
$$x_2(k) = \eta_2(k). \tag{3. 5}$$

In this case the signal received at sonabuoy 2 consists entirely of noise and the frequency domain representation of the two signals is thus:

$$X_1(\omega) = S(\omega) + N_1(\omega)$$
$$X_2(\omega) = N_2(\omega). \tag{3. 6}$$

## B. MOMENTS AND CUMULANTS OF A RANDOM PROCESS

For the purposes of this thesis, the following notation and definitions are used. The $n^{th}$ moment of a real stationary random process is [Ref 7:p. 15]

$$m_x^n(\tau_1, \tau_2, ..., \tau_{n-1},) = E\{x(k)x(k+\tau_1)...x(k+\tau_{n-1})\}, \quad (3.7)$$

where $E$ denotes statistical expectation and $\tau_i$ represents the $i^{th}$ lag. Note that $m_x^2(\tau)$ is the ordinary autocorrelation function .

In the analysis of signals using higher order statistics, cumulants rather than moments are generally used. Cumulants of order $n$ are defined by certain linear combinations of products of moments of order $n$ and lower [Ref 7:p. 15]. Cumulants of Gaussian random processes have the distinction that they are all zero for order $n$ greater than 2. Thus signals imbedded in additive gaussian noise theoretically appear naked when subjected to analysis using higher order cumulants. The $n^{th}$ order cumulant is denoted by

$$c_x^n(\tau_1, \tau_2, ....., \tau_{n-1},) = Cum[x(k)x(k+\tau_1)...x(k+\tau_{n-1})] \quad (3.8)$$

For a more detailed definition of cumulants the reader is referred to [Ref 7:p. 9].

The following relationships exist between moments and cumulants for stationary random processes [Ref 7:p. 9]:

***a. First Order.***

$$c_x^1 = m_x^1 = E\{x(k)\} \quad (3.9)$$

***b. Second Order.***

$$c_x^2(\tau_1) = m_x^2(\tau_1) - (m_x^1)^2 \quad (3.10)$$

***c. Third Order***

$$c_x^3(\tau_1, \tau_2) = m_x^3(\tau_1, \tau_3) - (m_x^1)\left[m_x^2(\tau_1) + m_x^2(\tau_2) + m_x^2(\tau_2 - \tau_1)\right] + 2(m_x^1)^3 \quad (3.11)$$

Using these relationships, zero mean, white Gaussian noise has the characteristics listed in Table 1.

| $n$ | $m^n$ | $c^n$ |
|---|---|---|
| 1 | 0 | 0 |
| 2 | $\sigma^2$ | $\sigma^2$ |
| 3 | 0 | 0 |
| 4 | $3\sigma^4$ | 0 |

**Table 1. Moments and cumulants for white gaussian noise for $\tau_1 = \tau_2 = \tau_3 = 0$.**

## C. N-TH ORDER "MOMENTS" OF A DETERMINISTIC SIGNAL

In this thesis, we consider transients to be deterministic signals. Consequently, concepts such as statistical moments are not defined. However certain operations in the time domain, which are analogous to estimating moments for realizations of a random process, are still useful for deterministic signals. Some authors (e.g., Nikias and Petropulu [Ref 7]) have referred to these operations as computing "moments and higher order spectra for deterministic signals." Since some of the techniques we have adapted are due to authors using this concept, we will adopt this concept here as well.

In general the $n^{th}$ order moment for an energy signal, $x(k)$, is defined as [Ref 7:p. 78]

$$m_x^n(\tau_1,....\tau_{n-1}) = \sum_{k=-\infty}^{\infty} x(k)x(k+\tau_1)...x(k+\tau_{n-1}), \tag{3. 12}$$

and for a power signal [Ref 7:p. 100] as

$$m_x^n(\tau_1,....\tau_{n-1}) = \frac{1}{N}\sum_{k=J}^{J+N-1} x(k)x(k+\tau_1)....x(k+\tau_{n-1}), \tag{3. 13}$$

where $J$ is an arbitrary starting point of the summation and $N$ is the period of the signal. From these expressions, moments can be considered as a measure of the degree of similarity between a signal and delayed or advanced replicas of itself. The $n^{th}$ order cross moment for $n$ energy signals is defined as

$$m^n_{x_1x_2....x_n}(\tau_1,...,\tau_{n-1}) = \sum_{k=-\infty}^{\infty} x_1(k)x_2(k+\tau_1)...x_n(k+\tau_{n-1}) \tag{3. 14}$$

The $n^{th}$ order moment spectrum is the Fourier transform of Eq. 3.12 and can be expressed as Fourier transforms of the signal. For energy signals, this is given by [Ref 7:p.85]

$$M_x^n(\omega_1,...\omega_{n-1}) = X(\omega_1)..X(\omega_{n-1})X^*(\omega_1+..+\omega_{n-1}), \tag{3. 15}$$

which can be written in terms of magnitude and phase as

$$\begin{aligned} \left|M_x^n(\omega_1,...\omega_{n-1})\right| &= \left| X(\omega_1)\right|..\left| X(\omega_{n-1})\right|\left| X(\omega_1+..+\omega_{n-1})\right| \\ \Psi_x^n(\omega_1,...\omega_{n-1}) &= \phi(\omega_1)+...+\phi(\omega_{n-1})-\phi(\omega_1..,\omega_{n-1}), \end{aligned} \tag{3. 16}$$

where $\left|M_x^n(\omega_1,...\omega_{n-1})\right|$ is the magnitude term and $\Psi_x^n(\omega_1,...\omega_{n-1})$ is the phase term. Orders *n=2, 3* and *4* are important special cases of moments. In the frequency domain these orders have been termed Power Spectral Density (PSD), Bispectrum, and Trispectrum, respectively.

## D. SECOND-ORDER MOMENTS

### 1. Definitions of Moments and Spectra

Using Eq 3.12, the autocorrelation of a deterministic signal, $x(k)$, is written as

$$m_x^2(\tau) = \sum_{k=-\infty}^{\infty} x(k)x(k+\tau). \tag{3. 17}$$

From Eq 3.16, the magnitude and phase components of the PSD are given by

$$\begin{aligned} \left|M_x^2(\omega)\right| &= \left|X(\omega)\right|^2 \\ \Psi_x^2(\omega) &= 0. \end{aligned} \tag{3. 18}$$

From these expressions, it can be seen that the PSD is an even function with no phase information. Similarly, the cross-correlation of two deterministic signals is

$$m_{x_1x_2}^2(\tau) = \sum_{k=-\infty}^{\infty} x_1(k)x_2(k+\tau). \tag{3. 19}$$

The corresponding cross-spectrum is the Fourier transform of Eq 3.19:

$$M_{x_1x_2}^2(\omega) = X_1(\omega)X_2^*(\omega), \tag{3. 20}$$

which can be written in terms of magnitude and phase

$$\left|M^2_{x_1x_2}(\omega)\right| = \left|X_1(\omega)\right|\left|X_2(\omega)\right|$$
$$\Psi^2_{x_1x_2}(\omega) = \phi_{x_1}(\omega) - \phi_{x_2}(\omega). \qquad (3.\ 21)$$

## 2. Second Order Moments of the Received Signals

Since cross-correlation is used extensively throughout the thesis, it is important to determine the cross-correlations for the three signal cases presented earlier. Before doing this, let us first investigate the cross-correlation between the two noise sources $\eta_1(k)$ and $\eta_2(k)$ at the two sonabuoys of interest. The cross-correlation and the corresponding cross-spectrum are given by:

$$m^2_{\eta_1\eta_2}(\tau) = \sum_{k=-\infty}^{\infty} \eta_1(k)\eta_2(k+\tau)$$
$$M^2_{\eta_1\eta_2}(\omega) = \Im\left\{m^2_{\eta_1\eta_2}(\tau)\right\} = N_1(\omega)N_2(\omega). \qquad (3.\ 22)$$

The expectation of this term is zero since the two white noise sources are uncorrelated. However, the term, $M^2_{\eta_1\eta_2}$, itself is not zero. Applying this to the case where the same transient arrives at the two sonabuoys, the cross spectrum is

$$M^2_{x_1x_2}(\omega) = \left|S(\omega)\right|^2 e^{-j\omega L} + M^2_{\eta_1\eta_2}(\omega) + M^2_{x\eta}(\omega), \qquad . \quad (3.\ 23)$$

where $M^2_{x\eta}$ are the cross terms. From this equation, it can be seen that the time delay $L$ is imbedded in the linear phase term $e^{-j\omega L}$. This linear phase term is therefore important in finding the TDOA between the two signals.

For the case where different transients arrive at the two sonabuoys, the cross-spectrum is

$$M^2_{x_1x_2}(\omega) = \left|S(\omega)\right|\left|R(\omega)\right|e^{j(\phi_S(\omega)-\phi_R(\omega))}e^{-j\omega L} + M^2_{\eta_1\eta_2}(\omega) + M^2_{x\eta}(\omega). \qquad (3.\ 24)$$

For this case it can be seen that there is the same linear phase term $e^{-j\omega L}$ as that of Eq 3.24. Therefore the same TDOA result would be observed for Eq 3.24 and 3.25 even though the transients are different. The linear phase can therefore not be used as a means to discriminate between two transients. In the last case, where there is only noise present, the cross-correlation is

$$M^2_{x_1x_2}(\omega) = M^2_{\eta_1\eta_2}(\omega). \qquad (3.\ 25)$$

For this case, it is expected that the phase will be random, and therefore no linear phase term will exist.

## E. THIRD-ORDER MOMENTS – BICORRELATION AND BISPECTRUM

### 1. Definition of Moments and Spectra

The third-order moment of a signal is called the *bicorrelation*. From Eq 3.12, the auto-bicorrelation of a deterministic real signal is defined as

$$m_x^3(\tau_1,\tau_2)=\sum_{k=-\infty}^{\infty} x(k)x(k+\tau_1)x(k+\tau_2) \tag{3.26}$$

and from Eq 3.14 the cross bicorrelation is

$$m_{x_1x_2x_3}^3(\tau_1,\tau_2)=\sum_{k=-\infty}^{\infty} x_1(k)x_2(k+\tau_1)x_3(k+\tau_2). \tag{3.27}$$

For this thesis, where there are only two data streams, the cross-bicorrelation will consist of only two signals, $x_1(k)$ and $x_2(k)$. The cross-bicorrelation functions of interest are

$$m_{x_1x_1x_2}^3(\tau_1,\tau_2)=\sum_{k=-\infty}^{\infty} x_1(k)x_1(k+\tau_1)x_2(k+\tau_2) \tag{3.28}$$

and the terms $m_{x_1x_1x_2}^3$, $m_{x_2x_1x_1}^3$ and $m_{x_1x_2x_1}^3$, which are defined in an analogous way.

The auto-bispectrum is

$$M_x^3(\omega_1,\omega_2)=X(\omega_1)X(\omega_2)X^*(\omega_1+\omega_2), \tag{3.29}$$

or in terms of magnitude and phase

$$\begin{aligned}\left|M_x^3(\omega_1,\omega_2)\right| &= \left|X(\omega_1)\right|\left|X(\omega_2)\right|\left|X(\omega_1+\omega_2)\right| \\ \Psi_x^3(\omega_1,\omega_2) &= \phi_x(\omega_1)+\phi_x(\omega_2)-\phi_x(\omega_1+\omega_2).\end{aligned} \tag{3.30}$$

As can be seen, by comparing Eq 3.18 and Eq 3.30, a distinct difference between the second order moment spectrum and the bispectrum is that the bispectrum contains phase information. The cross-bispectrum is

$$M_{x_1x_2x_3}^3(\omega_1,\omega_2)=X_2(\omega_1)X_3(\omega_2)X_1^*(\omega_1+\omega_2), \tag{3.31}$$

or in terms of magnitude and phase

$$\left|M^3_{x_1x_2x_3}(\omega_1,\omega_2)\right| = \left|X_2(\omega_1)\right|\left|X_3(\omega_2)\right|\left|X_1(\omega_1+\omega_2)\right|$$
$$\Psi^3_{x_1x_2x_3}(\omega_1,\omega_2) = \phi_{x_2}(\omega_1)+\phi_{x_3}(\omega_2)-\phi_{x_1}(\omega_1+\omega_2). \tag{3.32}$$

## 2. Third Order Moments of the Received Signals

Both second order moments and third order moments are used extensively throughout this thesis. It is therefore important to develop the third order moments for the three signal cases. To provide a motivation for the algorithms to be used, let us consider a situation in which the noise is identically zero. In reality the noise terms $N_1(\omega)$ and $N_2(\omega)$ are not zero, although the expected value of their higher order moments defined earlier vanish when the noise is Gaussian.

For the case where the same transient arrives at both sonabuoys, the signals in the frequency domain are given by Eq. 3.2. Using Eq. 3.32, the bispectrum of these signals is given by

$$\left|M^3_{x_1x_2x_1}(\omega_1,\omega_2)\right| = \left|S(\omega_1)\right|\left|S(\omega_2)\right|\left|S(\omega_1+\omega_2)\right|$$
$$\Psi^3_{x_1x_2x_1}(\omega_1,\omega_2) = \phi_S(\omega_1)-\omega L+\phi_S(\omega_2)-\phi_S(\omega_1+\omega_2), \tag{3.33}$$

where $\phi_S$ is the phase of the signal $S(\omega)$. Equation 3.33 is the expression for the cross-bispectrum between the data streams at sonabuoy 1 and sonabuoy 2 in the absence of noise. The signal phase terms, $\phi_S(\omega_1)+\phi_S(\omega_2)-\phi_S(\omega_1+\omega_2)$, can be eliminated by making use of the auto-bispectrum at sonabuoy 1, which is given by

$$\left|M^3_{x_1}(\omega_1,\omega_2)\right| = \left|S(\omega_1)\right|\left|S(\omega_2)\right|\left|S(\omega_1+\omega_2)\right|$$
$$\Psi^3_{x_1}(\omega_1,\omega_2) = \phi_S(\omega_1)+\phi_S(\omega_2)-\phi_S(\omega_1+\omega_2). \tag{3.34}$$

This expression is then used to normalize the cross-bispectrum and results in the identity:

$$I(\omega_1,\omega_2) = \frac{M^3_{x_1x_2x_1}(\omega_1,\omega_2)}{M^3_{x_1}(\omega_1,\omega_2)} = e^{-j\omega_1 L}. \tag{3.35}$$

From Eq 3.35 it can be seen that by normalizing the bispectrum all the phase terms are cancelled except for the linear phase term, $e^{-j\omega_1 L}$.

For the case of different transient arrivals, the cross-bispectrum can be obtained from Eq. 3.4 and Eq. 3.32 as follows

$$\begin{aligned} \left|M_{x_1x_2x_1}(\omega_1,\omega_2)\right| &= \left|R(\omega_1)\right|\left|S(\omega_2)\right|\left|S(\omega_1+\omega_2)\right| \\ \Psi_{x_1x_2x_1}(\omega_1,\omega_2) &= \phi_R(\omega_1)-\omega L+\phi_S(\omega_2)-\phi_S(\omega_1+\omega_2), \end{aligned} \tag{3.36}$$

where $\phi_R(\omega)$ is the phase of the signal $R(\omega)$. In this case the normalized cross-bispectrum takes the form

$$I(\omega_1,\omega_2)=\frac{M^3_{x_1x_2x_1}(\omega_1,\omega_2)}{M^3_{x_1}(\omega_1,\omega_2)}=\frac{\left|R(\omega_1)\right|}{\left|S(\omega_1)\right|}e^{j(\phi_R(\omega_1)-\phi_S(\omega_1))}e^{-j\omega_1 L}. \tag{3.37}$$

Note that, unlike the first case (see Eq. 3.35), the linear phase term cannot be separated from the other phase terms. In both cases however, the two-dimensional bispectrum is reduced to a function of a single variable $\omega_1$.

## F. SIGNAL PROCESSING ALGORITHMS

### 1. Bispectrum Linear Phase Detector

The analysis of the previous section shows that when the same signal is arriving at both sonabuoys, a linear phase term is present in the normalized function $I(\omega_1,\omega_2)$. The time delay $L$ can now be extracted using the following *ad hoc* method developed for time delay estimation [Ref 16].

To estimate the delay $L$, a third-order "hologram" transformation is required. This is defined to be [Ref 7:p. 324]

$$T(\tau)=\int_{-\pi}^{\pi}\int_{-\pi}^{\pi} I(\omega_1,\omega_2)e^{-j\omega_1\tau}\,d\omega_1 d\omega_2. \tag{3.38}$$

Since $I$ reduces the bispectrum to one dimension, the third-order hologram is a one-dimensional Fourier transform over the dimension containing the linear phase term, followed by an integration over the second dimension. Note that when the same signal is present at both sonabuoys, Eq. 3.38 takes the form

$$T(\tau) = \int_{-\pi}^{\pi}\int_{-\pi}^{\pi} e^{j\omega_1(L-\tau)} d\omega_1 d\omega_2. \qquad (3.39)$$

Since all the elements of this second dimension are in phase they add up constructively, giving a strong peak at $\tau = L$. Since we are working in the discrete-time domain the third-order hologram can be rewritten as

$$\hat{T}(\tau) = \sum_{\omega_1=0}^{M-1}\sum_{\omega_2=0}^{M-1} I(\omega_1, \omega_2) e^{-j\omega_1\tau}. \qquad (3.40)$$

The absolute value of $\hat{T}(\tau)$ will display a strong peak at the location of the of the time delay between the two signals of sonabuoy 1 and sonabuoy 2.

For the case where the two transient arrivals are different, the third-order hologram takes the form:

$$T(\tau) = \int_{-\pi}^{\pi}\int_{-\pi}^{\pi} \frac{|R(\omega_1)|}{|S(\omega_1)|} e^{j\omega_1(L-\tau)} e^{j(\phi_R(\omega_1)-\phi_S(\omega_1))} d\omega_1 d\omega_2. \qquad (3.41)$$

In this case, the third order hologram contains extra phase terms $\phi_R$ and $\phi_S$, which will either add in phase or out of phase. Thus, in general, $\hat{T}(\tau)$ will not exhibit a strong peak.

### 2. Bispectrum Discriminator

The bispectrum linear phase detector can also be used as a discriminator by applying a simple threshold technique to the third order hologram. The threshold technique is applied by first noticing, from Eq 3.41, that if the transients are different the hologram contains phase terms $\phi_R$ - $\phi_S$ -$\omega L$ and magnitudes $\frac{|R(\omega_1)|}{|S(\omega_1)|}$. On the other hand, if the transient signals are the same, the hologram contains only the linear phase term $\omega L$ (Eq 3.39). The phase and magnitude terms of Eq 3.41 will add constructively or destructively to produce peaks and valleys to the bispectral hologram. If the signals are the same, there will be only one peak in the hologram, and that peak will be at the delay $L$.

In summary, one can expect that if the SNR is sufficiently large and the signals are the same, a peak at delay $L$ will dominate the hologram. On the other hand if the signals are different, there will be a maximum value at delay $L$ as well as other extrema at

delays other than $L$. These other extrema will be larger than the noise and can therefore be used to discriminate. A discrimination algorithm is therefore proposed as follows:

Step 1:

Estimate $\hat{T}(\tau)$

Step 2:

Find the maximum value of the hologram

$$Q = \arg\max_{\tau}\left(\hat{T}(\tau)\right) \tag{3. 42}$$

($Q$ is the magnitude of the hologram at the estimated TDOA).

Step 3:

If $\tau_0$ is the value of $\tau$ that produces the maximum in step 2 then compute

$$Q_2 = \arg\max_{\substack{\tau \\ \tau \neq \tau_o}}\left(\hat{T}(\tau) - Q\right). \tag{3. 43}$$

Step 4:

Define a threshold using Eqs. 3.42 and 3.43 as

$$Q_T = \frac{1}{N-2}\left(\sum_{i=0}^{N-1}\hat{T}(\tau) - Q - Q_{2^{nd}}\right). \tag{3. 44}$$

Step 5:

Compare $Q_T$ to the difference $Q - Q_2$. If

$$Q_T > Q - Q_2 \tag{3. 45}$$

the signals are considered to be different; if

$$Q_T < Q - Q_2 \tag{3. 46}$$

the two signals are considered to be the same.

THIS PAGE INTENTIONALLY LEFT BLANK

# IV. SUBSPACE-BASED SIGNAL PROCESSING

Signal subspace methods have been used in a variety of problems for estimating spectral lines and direction of arrival in sensor arrays. A good introduction to these methods for spectrum estimation can be found in [Ref 17]. Recently, the use of subspace methods has been explored for estimating TDOA [Ref 20], [Ref 21]. This thesis uses the same approach as [Ref 20] for TDOA estimation and further adapts the subspace method for transient discrimination.

The discussion begins by defining the subspace model for the TDOA problem and then moves on to the MUSIC method, which was used for delay estimation and discrimination. The chapter finishes with a discussion of how the MUSIC method was adapted and used for discrimination

## A. SUBSPACE

To understand the principle of subspace methods and their application to the topic of this thesis, consider the case where the same signal is arriving at two separate sonabuoys (see Eq. 3.1). The frequency domain representation of Eq. 3.1 is given by Eq 3.2. From Eq. 3.2, it can be seen that the linear phase term $e^{-j\omega L}$ contains the delay $L$ between the transient arrivals at sonabuoy 1 and sonabuoy 2. The cross-spectrum for the two received signals, given by Eq 3.23, is repeated here for convenience

$$M^2_{x_1x_2}(\omega) = |S(\omega)|^2 e^{-j\omega L} + M^2_{\eta_1\eta_2}(\omega) + M^2_{x\eta}(\omega). \qquad (4.1)$$

It can be argued [see Ref 20] that when Eq 4.1 is sampled at equally-spaced values in frequency, the resulting data sequence, $y(k) = M^2_{x_1x_2}(\omega_k)$, satisfies the conditions necessary to apply a signal subspace model [Ref 17]. Specifically, an $N \times N$ correlation matrix is estimated for the data $y(k)$, and the corresponding $N$-dimensional vector space is divided into signal and noise subspaces. The approach followed to estimate TDOA using subspace methods is to project a steering vector of the form

$$\mathbf{d}(l) = \begin{bmatrix} 1 \\ e^{jl} \\ . \\ . \\ e^{jl(N-1)} \end{bmatrix} \tag{4. 2}$$

onto the noise subspace and plot the result as the linear phase, $l$, is varied. When the parameter $l$ is equal to the true delay $L$ between the sonabuoys, the projection onto the noise space is zero. In subspace algorithms, such as MUSIC, this null projection can be used to estimate TDOA.

Unfortunately, the cross-spectrum for the case where different transients are arriving at sonabuoys 1 and 2 also contains a linear phase term (see Eq. 3.24). Therefore, the basic subspace techniques are not useful for transient discrimination without suitable modification.

## B. MUSIC

In the application of subspace techniques to linear phase detection between two transients, the MUSIC (Multiple Signal Classification) method developed by Schmidt [Ref 18] is used. A brief outline of the method is provided here.

The MUSIC algorithm is implemented in the frequency domain by first obtaining the cross-spectrum of the two signals received at the sonabuoys. Since $M^2_{x_1x_2}(\omega)$ is formed using a DFT, this data is available at samples $\omega_k$, $k= 0,1,2...N_{DFT}-1$, where $N_{DFT}$ is the size of the DFT. From this frequency domain data, a data matrix[2] $\mathbf{M}^2_{x_1x_2}$ is formed, and the correlation matrix is estimated as

$$\mathbf{R}_x = \mathbf{M}^2_{x_1x_2}\left(\mathbf{M}^2_{x_1x_2}\right)^{*T}. \tag{4. 3}$$

This can be decomposed into an orthonormal eigenvector matrix

$$\mathbf{E} = [\mathbf{E}_{sig}\mathbf{E}_{noise}] \tag{4. 4}$$

and a diagonal eigenvalue matrix

[2] See [Ref 17] for various methods of forming a data matrix

$$\Lambda = \begin{bmatrix} \Lambda_{sig} & 0 \\ 0 & \Lambda_{noise} \end{bmatrix}. \tag{4. 5}$$

The columns of $\mathbf{E}_{sig}$ and $\mathbf{E}_{noise}$ form an orthogonal basis set and define the signal and noise subspaces, respectively. It is therefore possible to write $\mathbf{R}_x$ as

$$\mathbf{R}_x = \mathbf{E}\Lambda\mathbf{E}^{*T} = \mathbf{E}_{sig}\Lambda_{sig}\mathbf{E}_{sig}^{*T} + \mathbf{E}_{noise}\Lambda_{noise}\mathbf{E}_{noise}^{*T}. \tag{4. 6}$$

The columns of the eigenvector matrix can be used to form projection matrices for the signal and noise subspaces of the form [Ref 17:p. 623]:

$$\begin{aligned} \mathbf{P}_{sig} &= \mathbf{E}_{sig}\mathbf{E}_{sig}^{*T} \\ \mathbf{P}_{noise} &= \mathbf{E}_{noise}\mathbf{E}_{noise}^{*T}. \end{aligned} \tag{4. 7}$$

When the projection matrix $\mathbf{P}$ is multiplied by a vector $\mathbf{d}$, the result $\hat{\mathbf{d}} = \mathbf{P}\mathbf{d}$ is the projection of $\mathbf{d}$ into the corresponding subspace (see Figure 5).

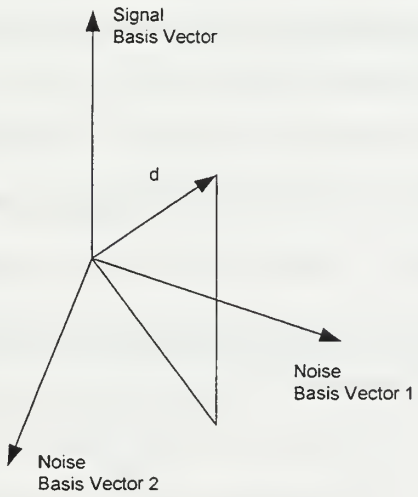


**Figure 5. Projection of vector d onto noise subspace by MUSIC.**

As discussed previously, subspace methods make use of the fact that the projection of the steering vector $\mathbf{d}(l)$ , given by Eq. 4.2 onto the noise subspace is zero. The MUSIC algorithm [Ref 17:p. 627], in particular, evaluates the quantity

$$\hat{P}_{MU} = \frac{1}{\mathbf{d}^{*T}(l)\mathbf{P}_{noise}\mathbf{d}(l)} = \frac{1}{\mathbf{d}^{*T}(l)\sum_{i=2}^{N}\mathbf{e}_i\mathbf{e}_i^{*T}\mathbf{d}(l)}, \tag{4. 8}$$

where $\hat{P}_{MU}$ is the MUSIC indicator function for $\mathbf{d}(l)$and $\mathbf{e}_2 ... \mathbf{e}_N$ are the eigenvetors spanning the noise subspace (the eigenvector $\mathbf{e}_1$ spans the signal-subspace which is one-dimensional) The value of $l$ where $\hat{P}_{MU}$ exhibits a sharp peak determines the TDOA between the signals.

## C. SUBSPACE DISCRIMINATOR

A subspace discriminator was developed by comparing projections onto multiple subspaces using the MUSIC algorithm. The following considerations are proposed to motivate this discriminator.

Since the subspace method in this thesis is based on the cross-spectrum between two sonabuoys (see Eq. 4.1) it is important to investigate the differences between the cross-spectrum for the case where the same transient arrives at two separate buoys and that for the case where different transients arrive at two separate buoys. This will be helpful in understanding the subspace discriminator. From Eq. 3.24, it can be seen that if the transients are different, the cross-spectrum contains phase terms $\phi_S(\omega) - \phi_R(\omega) - \omega L$ and magnitudes $|R(\omega_1)||S(\omega_1)|$. However, if the transient signals are the same, the cross-spectrum contains only the linear phase term $\omega L$ (Eq. 3.23). Now, if the subspaces formed using Eq. 3.23 are compared to those formed using Eq. 3.24 the two subspaces would typically be rotated with respect to each other as illustrated in Figure 6. The implication of the rotation of the subspaces due to the phase terms of Eq. 3.24 is that when the parameter $l$ of the steering vector, $\mathbf{d}(l)$, is equal to the delay L between the sonabuoys, the projection onto the noise subspace will not be zero as in the case when the same transient arrives at the two sonabuoys. By comparing projections, it would be found that the differences in magnitude of the projections would be large if the transients were the same. On the other hand if the transients were different, the differences in magnitude between the projections would be small. These differences in magnitude are used to discrimnate between transients.

This method is developed further by noticing that the noise projection matrix, $\mathbf{P}_{noise}$, can be written as:

$$\mathbf{P}_{noise} = \sum_{i=2}^{N} \mathbf{e}_i \mathbf{e}_i^{*T} = \mathbf{I} - \mathbf{e}_1 \mathbf{e}_1^{*T}, \tag{4. 9}$$

where $\mathbf{I}$ is an $N \times N$ identity matrix.Let us further define $\mathbf{P}_k$ as the projection operator for the subspace formed by leaving out the $k^{th}$ basis vector. Thus

$$\mathbf{P}_k = \sum_{\substack{i=1 \\ i \neq k}}^{N} \mathbf{e}_i \mathbf{e}_i^{*T} = \mathbf{I} - \mathbf{e}_k \mathbf{e}_k^{*T}. \tag{4. 10}$$

Further we define the following set of additional indicator functions

$$\hat{P}_k(l) = \frac{1}{\mathbf{d}^{*T}(l)\mathbf{P}_k \mathbf{d}(l)} = \frac{1}{\mathbf{d}^{*T}(l)[\mathbf{I} - \mathbf{e}_k \mathbf{e}_k^{*T}]\mathbf{d}(l)}, \quad k = 2,\ldots,N. \tag{4. 11}$$

The proposed subspace-based discrimination algorithm is as follows:

Step 1

Estimate the correlation matrix $\mathbf{R}_x$ and find the eigenvectors $\mathbf{e}_i$.

Step 2

Compute the maximum estimate

$$Q = \arg\max_{k,l} \left( \hat{P} \right). \tag{4. 12}$$

Step 3

If $k_0$ is the value of k that produces the maximum in step 2 then compute

$$Q_2 = \arg\max_{\substack{k,l \\ k \neq k_0}} \left( \hat{P} \right). \tag{4. 13}$$

Step 4

Compare the difference $Q - Q_2$. If

$$Q - Q_2 < 1 \tag{4. 14}$$

the signals are considered to be different. If

$$Q - Q_2 < 1 \tag{4. 15}$$

the signals are considered to be the same.

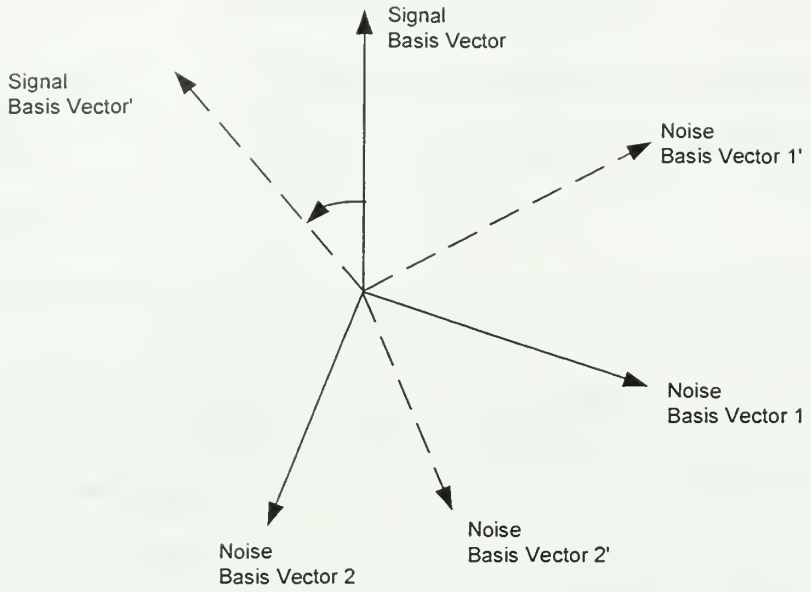


**Figure 6. Relative rotation of subspace due to phase terms of Eq. 3.24.**

# V. SIMULATION RESULTS

## A. SIMULATION CONDITIONS

### 1. Synthetic Transients

In this thesis a set of four synthetic transients was used to evaluate each of the algorithms described in the previous chapters. The four transients were a CW sinusoidal pulse, an exponentially decaying sinusoidal pulse, a linear phase modulated (LFM) pulse and a simulated finback whale transient.

Each transient can be described as an amplitude- and phase-modulated sinusoid, given by the general expression [Ref 19:p. 202]

$$p(t) = a(t)\cos\theta(t), \tag{5. 1}$$

where *a(t)* is the time-varying amplitude or "envelope" of the signal and *θ(t)* is the time-varying angle. The angle *θ(t)* is of the form $\theta(t) = 2\pi f_c t + \gamma(t)$ so that

$$p(t) = a(t)\cos(\omega_c t + \gamma(t)), \tag{5. 2}$$

where $f_c$ is the center frequency and *γ(t)* is the phase modulation. Each of these transients is described in more detail below.

For the CW pulse, the envelope and phase modulation are given by:

$$a(t) = \begin{cases} 1, & 0 \le t \le T \\ 0, & otherwise \end{cases} \tag{5. 3}$$

$$\gamma(t) = 0 \tag{5. 4}$$

where T is the pulse length. A plot of this transient is given in Figure 7 for $T = 40\,ms$ and $f_c = 50\,Hz$.

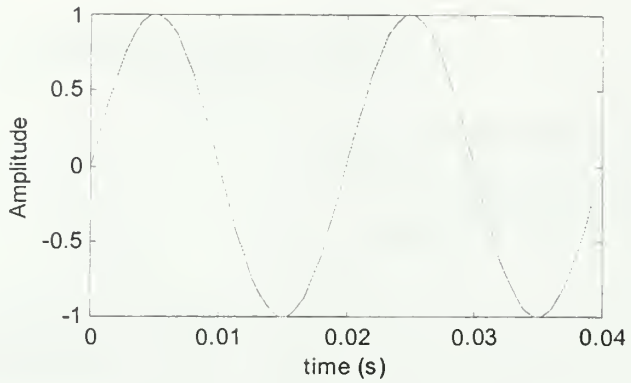


**Figure 7. CW Pulse.**

The exponentially decaying sinusoidal transient is described by the following envelope and phase modulation terms

$$a(t) = \begin{cases} e^{-\alpha t}, & 0 \le t \le T \\ 0, & otherwise \end{cases} \tag{5. 5}$$

$$\gamma(t) = 0, \tag{5. 6}$$

where $T$ is the pulse duration and $\alpha$ is the attenuation constant. This transient is shown in Figure 8 for $\alpha = 200$ and $T = 40ms$.

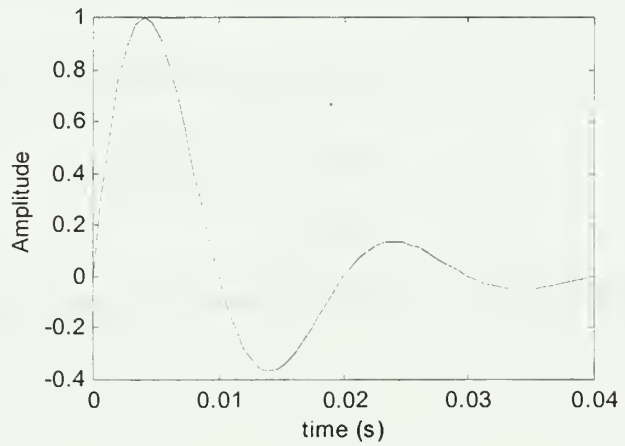


**Figure 8. Exponentially Decaying Sinusoidal Transient.**

For the Linear Phase Modulated (LFM) transient, a Gaussian envelope of the form

$$a(t)=\begin{cases} e^{\left(t-\frac{T}{2}\right)^2/2\sigma^2}, & 0<t<T \\ 0, & otherwise \end{cases} \tag{5. 7}$$

was used. The phase is a quadratic function of time:

$$\gamma(t)=\frac{2\pi\cdot\Delta f\cdot t^2}{2T} \tag{5. 8}$$

where $\Delta f$ is the desired change in instantaneous frequency over the interval $T$. A plot of this transient for $T = 40\,ms$ , $\sigma^2=\frac{T}{3}$ and $\Delta f = 100\,Hz$ is shown in Figure 9.

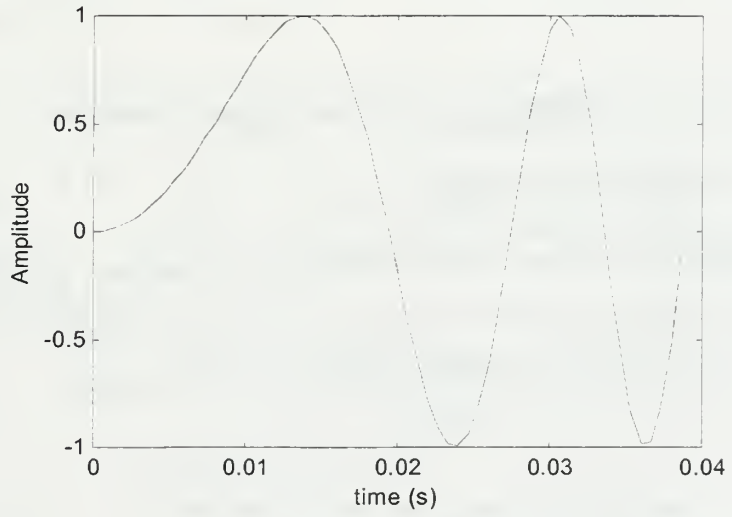


**Figure 9. LFM Pulse.**

The finback whale transient is the most complicated of all the transients that were synthesized. This transient is modeled as follows [Ref 8]:

$$a(t)=\begin{cases} (3/T)\cdot t, & 0<t<T/3 \\ 1, & T/3<t<2T/3 \\ 3-(3/T)\cdot t, & 2T/3<t<T \\ 0, & otherwise \end{cases} \tag{5. 9}$$

$$\gamma(t)=2\pi\cdot 23.e^{\ln(18\pi/23\pi)t} \tag{5. 10}$$

with $f_c$ = 0. This transient is plotted in Figure 10 for $T = 1\,s$. The instantaneous frequency decreases nonlinearly from 23 Hz to 18 Hz with the most rapid decrease occurring initially and the rate of decrease becoming smaller with time.

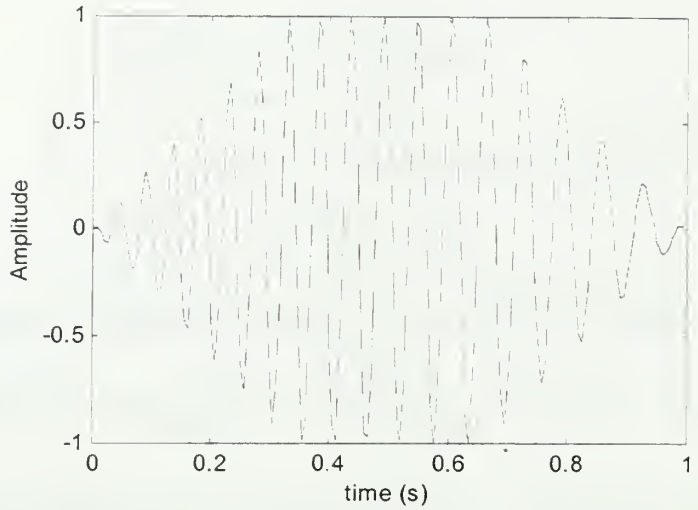


**Figure 10. Finback Whale Transient.**

### 2. Signal-to-Noise Ratio

During the evaluation of the algorithms, the synthetic signals described above were subject to additive white Gaussian noise. The signal-to-noise ratio (SNR) is defined as follows. Let $P_{transient}$ represent the average power in the signal:

$$P_{transient} = \frac{1}{N_s} \sum_{n=0}^{N_s-1} |x(n)|^2. \tag{5. 11}$$

Note that the transient signal power is normalized by the length of the transient $N_s$ and not the entire observation time. This is done to prevent the SNR from changing with changing observation time. The SNR in dB is then defined as

$$SNR = 10\log_{10} \frac{P_{transient}}{P_{Noise}} = 10\log_{10} \frac{P_{transient}}{\sigma^2_{noise}} dB \tag{5. 12}$$

where $\sigma^2_{noise}$ is the noise variance used in the generation of the Gaussian white noise.

## B. RESULTS

To evaluate the algorithms, two sets of experiments were used, one to perform TDOA estimation and the other to perform discrimination. For the first set of experiments, the same transient arrives at both sonabuoys. For this case all the transients were evaluated in turn, over a range of SNR values. For the second set of experiments,

all combinations of transient arrivals at sonabuoys 1 and sonabuoys 2 were tested for discrimination.

In all of the experiments, the transients were set to the following lengths: 20 ms for the CW sinusoidal pulse, 40 ms for the exponential decaying sinusoid and LFM pulse, and 1 s for the whale transient. The delay, $L$, between the transients was always kept at 40 samples, which is equivalent to 200ms. A sampling rate of four times the required Nyquist frequency was used for each transient. This satisfies the requirement for the bispectrum, which requires a sampling rate of three times the maximum frequency [Ref 8]. The total length of each signal used was 256 samples or 1.28 s. The parameters are summarized in Table 2.

| | $f_c$ (Hz) | $T$ | $L$ (delay) | $\Delta f$ | $\alpha$ |
|---|---|---|---|---|---|
| CW Pulse | 50 | 20ms | 200ms | | |
| Exponential Decaying Sinusoid | 50 | 40ms | 200ms | | 200 |
| LFM | 50 | 40ms | 200ms | 1kHz | |
| Whale | | 1s | 200ms | | |

**Table 2. Transient parameters used in experiments.**

### 1. TDOA Estimation

The TDOA results will be discussed as follows. First, an example of the basic results using the exponentially decaying sinusoid transient will be given for both the subspace method and the bispectrum linear phase detector. After this, certain "probability" curves for TDOA will be defined and presented for each transient starting with the subspace method and ending with the bispectrum results.

The subspace method uses the MUSIC algorithm with a correlation matrix (Eq. 4.3) of size $N = 60$. Figure 11 shows a plot of the function $\hat{P}_{MU}$ (see Eq. 4.8) as a function of $l$ using a SNR of 12 dB. Figure 12 is a plot of the results for a SNR of 5 dB.

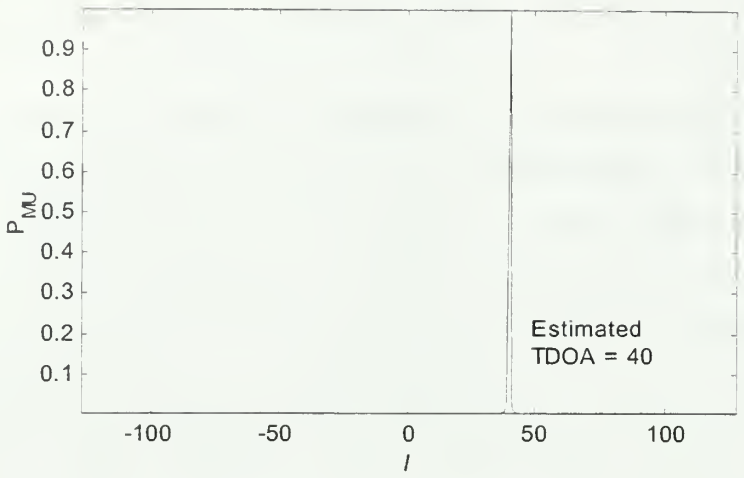


**Figure 11. Subspace TDOA estimation for an exponentially decaying sinusoid using an SNR of 12 dB and correlation matrix size of N=60.**

As can be seen from these figures, the algorithm estimates the correct TDOA of 40 samples or 200 ms for a SNR of 12 dB, and yields a completely incorrect value of –63 samples for an SNR of 5 dB.

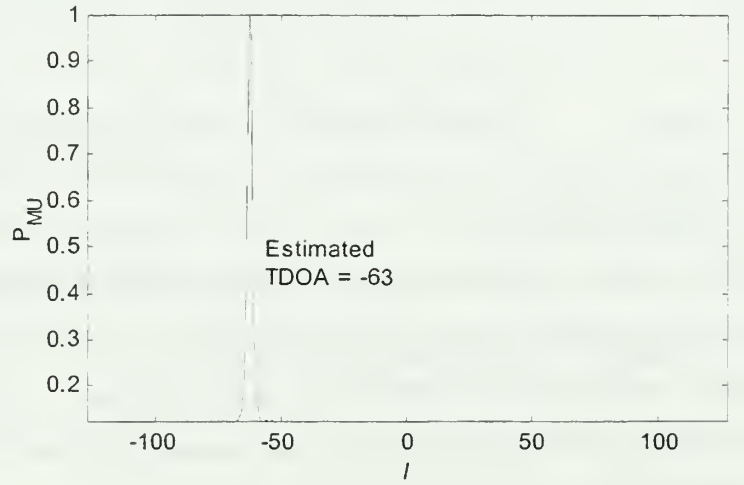


**Figure 12. Subspace TDOA estimation for an exponentially decaying sinusoid using an SNR of 5 dB and correlation matrix size of N=60.**

The rationale for using a large correlation matrix is twofold. First, if the correlation matrix is too small, the TDOA estimate tends to be less accurate. A typical result is shown in Figure 13 for the 12 dB-SNR case using a correlation matrix of size $N$

= 5. As can be seen in this figure, a TDOA of 38 samples (instead of the correct value 40 samples) was estimated, and the peak is broader than that shown in Figure 11. Secondly, for the subspace method to function as a discriminator, it was found that better results were achieved at lower SNR, when the correlation matrix and thus the observation space was larger.

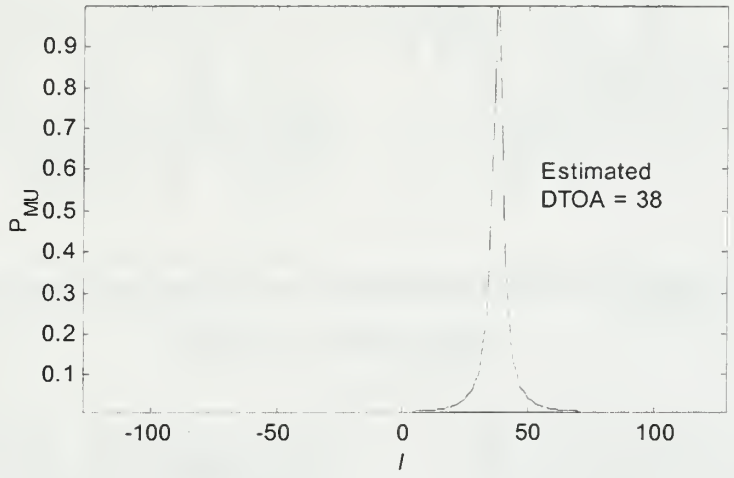


**Figure 13. Subspace TDOA estimation for an exponentially decaying sinusoid using an SNR of 12 dB and correlation matrix size of N = 5.**

For the bispectrum linear phase detector, no windowing was applied to the data. Windowing is usually applied to obtain smooth estimates of the bispectrum [Ref 7:p. 126]. Due to the short data lengths used in this thesis, however, it was found that windowing did not improve the results and was therefore not used. Typical results for the bispectrum linear phase detector are shown in Figure 14 and Figure 15 for the exponentially decaying sinusoid using SNR values of 12 dB and 5 dB. In both cases the TDOA is indicated by the maximum value of the hologram, which in turn is a single sample. The performance is similar to that of the subspace method. At 12 dB the result is exactly correct while at 5 dB the method gives completely erroneous results.

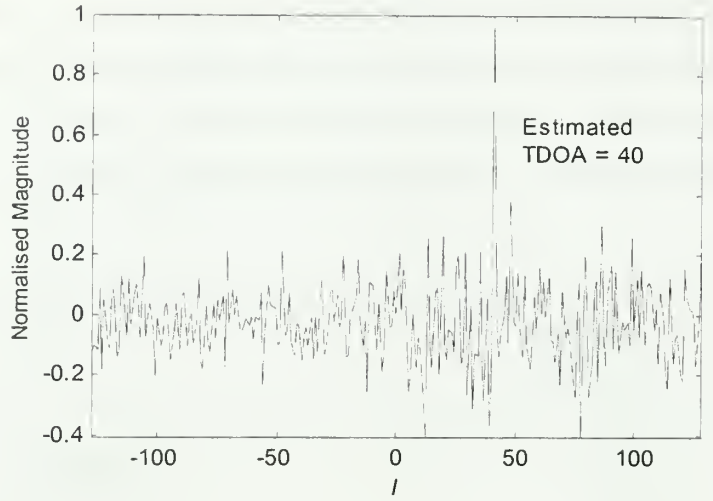


**Figure 14. Bispectrum TDOA estimation for an exponentially decaying transient using an SNR of 12 dB.**

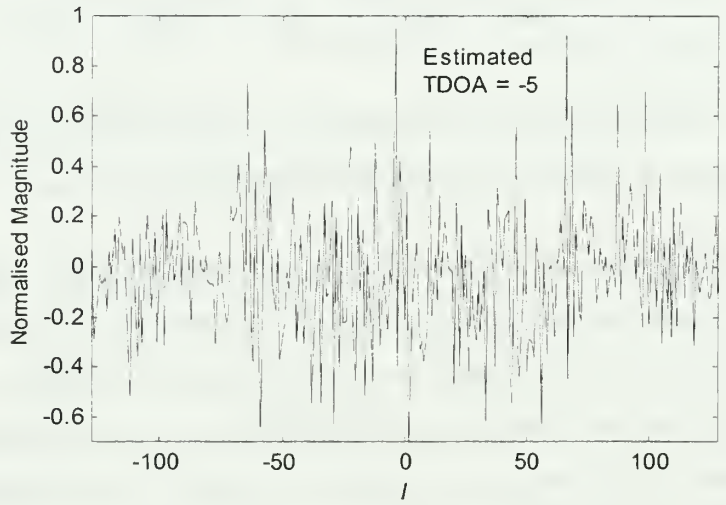


**Figure 15. Bispectrum TDOA estimation for an exponentially decaying transient using an SNR of 5 dB.**

Figure 16 shows typical TDOA results using the classical generalized cross-correlation methods (GCC) [Ref 2] at a SNR value of 12dB. ROTH [Ref 13], SCOT [Ref 14] and PHAT [Ref 15] weighting was used in addition to straight cross-correlation (no special weighting was used). As can be seen in Figure 16 the correlation, SCOT and PHAT algorithms give strong peaks at the estimated TDOA while ROTH gives a very

noisy signal with no dominant strong peak. In general, it was found that these techniques gave less accurate TDOA estimates than the bispectral and subspace algorithms, even at high SNRs.

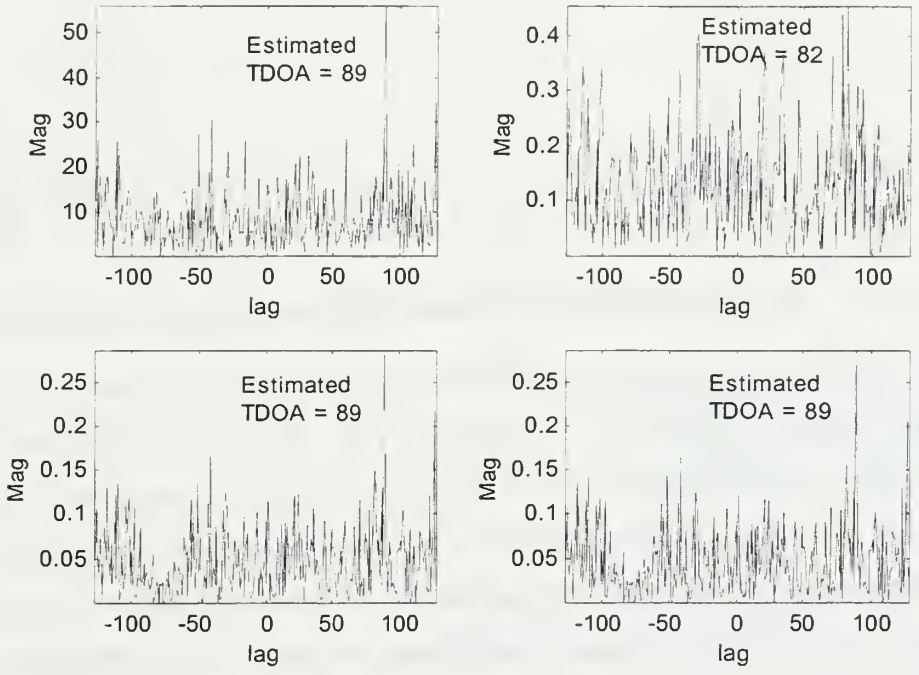


**Figure 16. TDOA estimates using (a) cross correlation, (b) ROTH, (c) SCOT and (d) PHAT with an SNR of 12 dB.**

TDOA-estimate performance of the subspace and bispectral algorithms was evaluated using simulations of one thousand realizations at a fixed SNR. For each realization, a different white noise source was added to the original signal. The output of these simulations was used to create a statistical measure of performance for TDOA, which we call the probability of correct TDOA $P_T$. $P_T$ represents the fraction of 1000 trials for which the algorithm estimates the correct time delay between transients received at the two sonabuoys. $P_T$ curves were generated for SNR values of 8 dB to 20 dB for both the subspace method and the bispectrum linear phase detector.

Figure 17 and Figure 18 (a) shows the $P_T$ results of the subspace algorithm for the CW pulse. As can be seen from the figures, the subspace algorithm gives excellent results for SNR > 17 dB, where a $P_T$ of 1.0 is achieved.

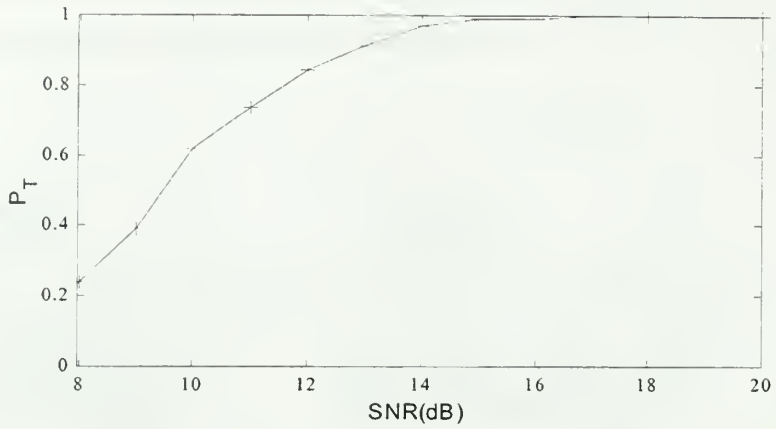


**Figure 17. $P_T$ versus SNR for CW pulse using the subspace linear phase detector.**

The $P_T$ curves for the exponentially decaying transient and the LFM transient are shown in Figure 18 (b) and (c). Once again, a $P_T$ value of 1.0 is achieved for SNR > 17dB. The $P_T$ for the whale transient (Figure 18 (d)) shows poorer results, achieving a maximum $P_T$ of 1.0 at a SNR of 20 dB. This poorer performance of the algorithm may be be attributed to two factors. First, the whale transient was the longest of all the transients used (being 1 s long) thus filling most of the data observation window. Secondly, it is a non-linear function giving it a complicated phase structure. It is also important to note that the results in Figure 18 (d) are based on a longer data observation length than used for the other TDOA results (see Table 3).

Figure 18 (a) and Figure 19 show the $P_T$ for the CW pulse using the bispectrum linear phase detector. From these figures, it can be seen that a $P_T$ of 1.0 is never achieved but that a $P_T$ of 0.9 is achieved at a SNR of 15 dB. The remaining plots in Figure 18 (b), (c) and (d) also show that a $P_T$ of 1.0 is not achieved for the bispectrum method. For the exponentially decaying sinusoid (Figure 18 (b)) a $P_T$ of 0.9 is achieved at 11 dB while for the LFM pulse (see Figure 18 (c)) a $P_T$ of 0.9 is achieved at 12 dB. As in the case of the subspace methods, the $P_T$ of the whale transient was obtained using a longer data observation window, where a maximum $P_T$ of 0.9 was achieved at an SNR of 16 dB (Figure 18(d) ).

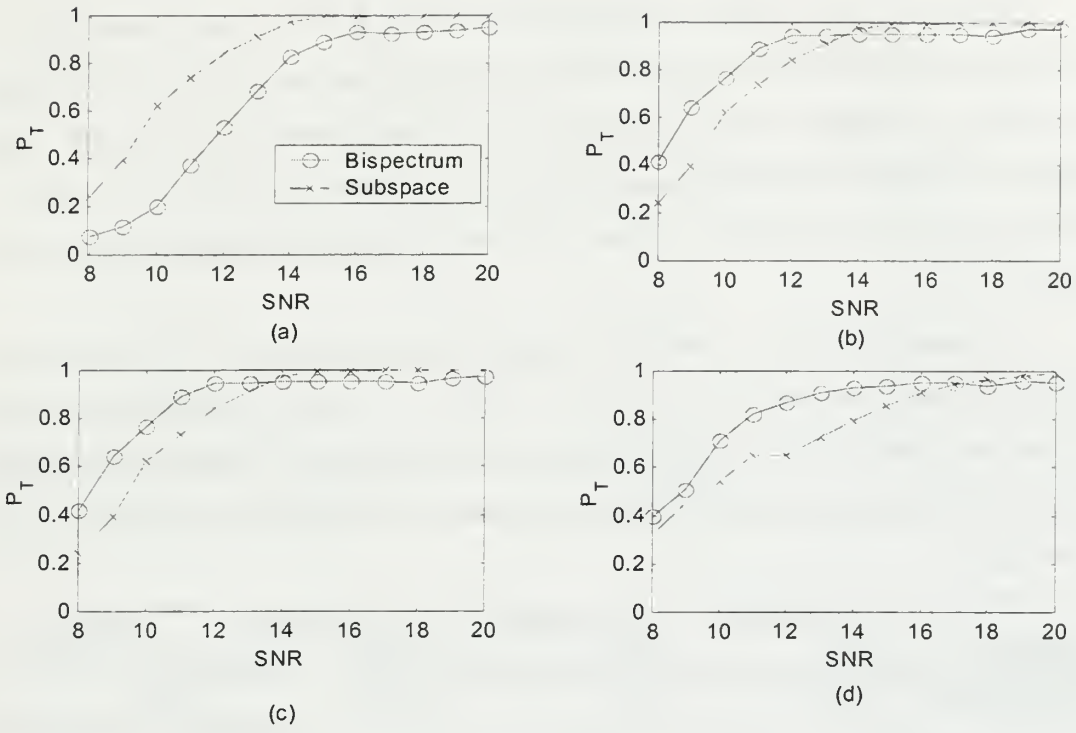


**Figure 18. Combined $P_T$ for subspace and bispectrum linear phase detectors: (a) CW pulse, (b) exponential decaying sinusoidal transient, (c) LFM pulse and (d) whale transient.**

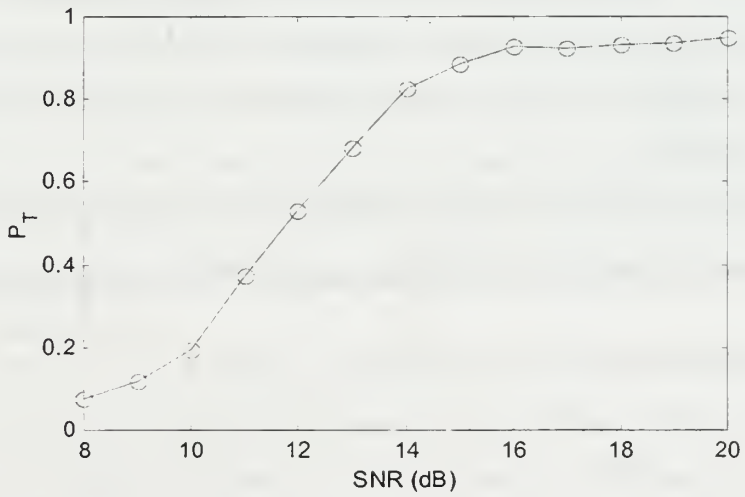


**Figure 19. $P_T$ for the CW pulse using the bispectrum linear phase detector.**

Figure 18 gives a summary of the TDOA results for all of the experiments. As can be seen in Figure 18, the bispectrum linear phase detector has higher $P_T$ values at low SNR than the subspace linear phase detector for the exponential, LFM and whale transients. However at higher values of SNR, the subspace algorithm gives better $P_T$ results (i.e., $P_T$ of 1.0) which is never achieved using the bispectrum linear phase detector.

In comparing the two methods (subspace and bispectrum) one may note that although the bispectrum method never achieves a $P_T$ of 1.0, in three out of the four cases it reaches the value of $P_T = 0.9$ earlier than the subspace method. Table 3 compares these results by listing the minimum SNR values for which a $P_T$ of 0.9 is achieved in each of the test cases.

| | CW Pulse | Exponential | LFM Pulse | Whale |
|---|---|---|---|---|
| **Subspace** | 13dB | 15dB | 14dB | 18dB |
| **Bispectrum** | 15dB | 11dB | 12dB | 16dB |

**Table 3. Minimum SNR required to achieve $P_T = 0.9$.**

### 2. Discrimination Experiments

The transient discrimination results will be discussed in a fashion similar to that of the TDOA results. The discussion will therefore start by giving a brief introduction of how the algorithms were implemented by using the CW and LFM pulses as examples. After this, the probability curves for discrimination will be discussed for every combination of transients.

As discussed previously, the subspace discriminator makes use of projections into multiple subspaces and compares the maximum values of the indicator functions $\hat{P}_k$ Eq. 4.11 with the maximum value of the function $\hat{P}_{MU}$ (Eq. 4.8). It is found that if the transients arriving at the sonabuoys are the same the difference in peak values will be large as shown in Figure 20(a). If the difference is found to be small (i.e., < 1) then the two transients are different, as shown in Figure 20(b). Thus in making these comparisons, it is possible to discriminate between transients.

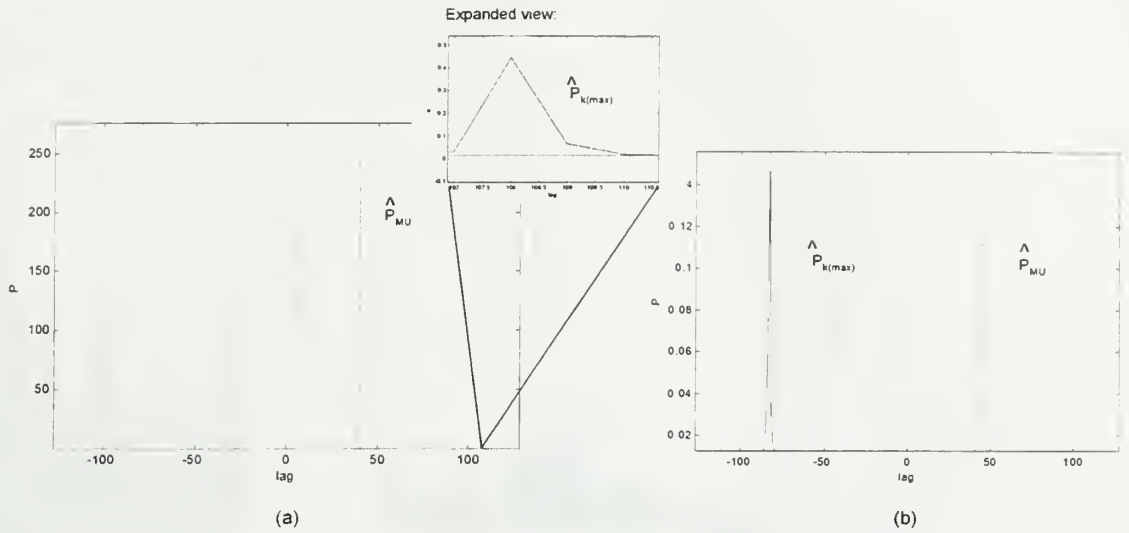


**Figure 20. Typical $\hat{P}_k$ estimates, (a) when the signals are the same and (b) when the signals are different.**

In the case of the bispectrum discriminator, the phase terms $\phi_R$ - $\phi_S$ (see Eq 3.37), which are only present in the case of different transient arrivals, add up constructively or destructively thus giving features to the hologram of the bispectral linear phase detector. For the case where the transients are the same, the phase terms $\phi_R$ - $\phi_S$ are zero; therefore no extra features are added to the hologram. If the difference in magnitude between these features is large compared to the average of the hologram, it is possible to discriminate between transients. These characteristics can be clearly seen in Figure 21. Figure 21(a) shows the single peak that appears for similar transient arrivals while Figure 21(b) shows the multiple peaks and extra features that are present due to the phase terms $\phi_R$ and $\phi_S$ for different transient arrivals.

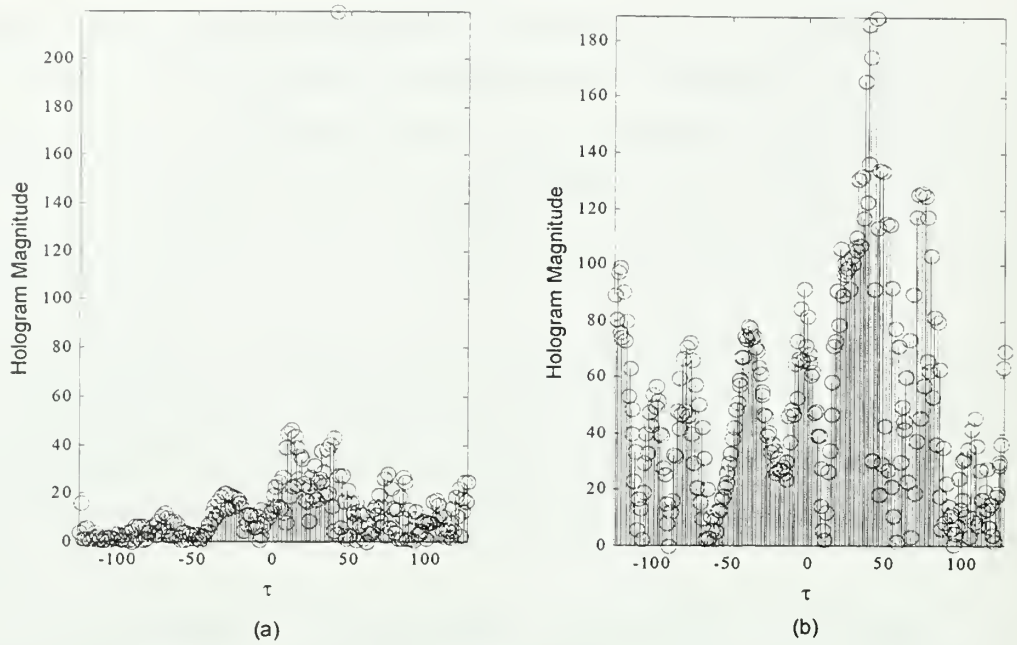


**Figure 21. Bispectrum linear phase detector. Stem plot of $|T(\tau)|$ for (a) similar transient arrivals and (b) different transient arrivals.**

The experiments for transient discrimination were as follows. Each algorithm was evaluated using simulations of one thousand realizations at a fixed SNR. For each realization, a different white noise source was added to the original signal. The output of these simulations was used to estimate the probability of correct discrimination ($P_{Di}$). $P_{Di}$ represents the fraction of 1000 trials for which the algorithm discriminates correctly between two transients. $P_{Di}$ curves were generated for SNR values of 10 dB to 20 dB for both the subspace and bispectrum discriminators. The probability of incorrect discrimination, $P_{fa}$, was computed in a similar manner and also used as a performance measure.

Figure 22 shows the results using the subspace discriminator where the exponentially decaying sinusoid is present at sonabuoy 1 and various transients are present at sonabuoy 2. For these curves, the vertical axis is labeled "Probability" because the $P_{fa}$ and $P_{Di}$ are shown on the same plot. In Figure 22, the $P_{Di}$ curve for the exponential

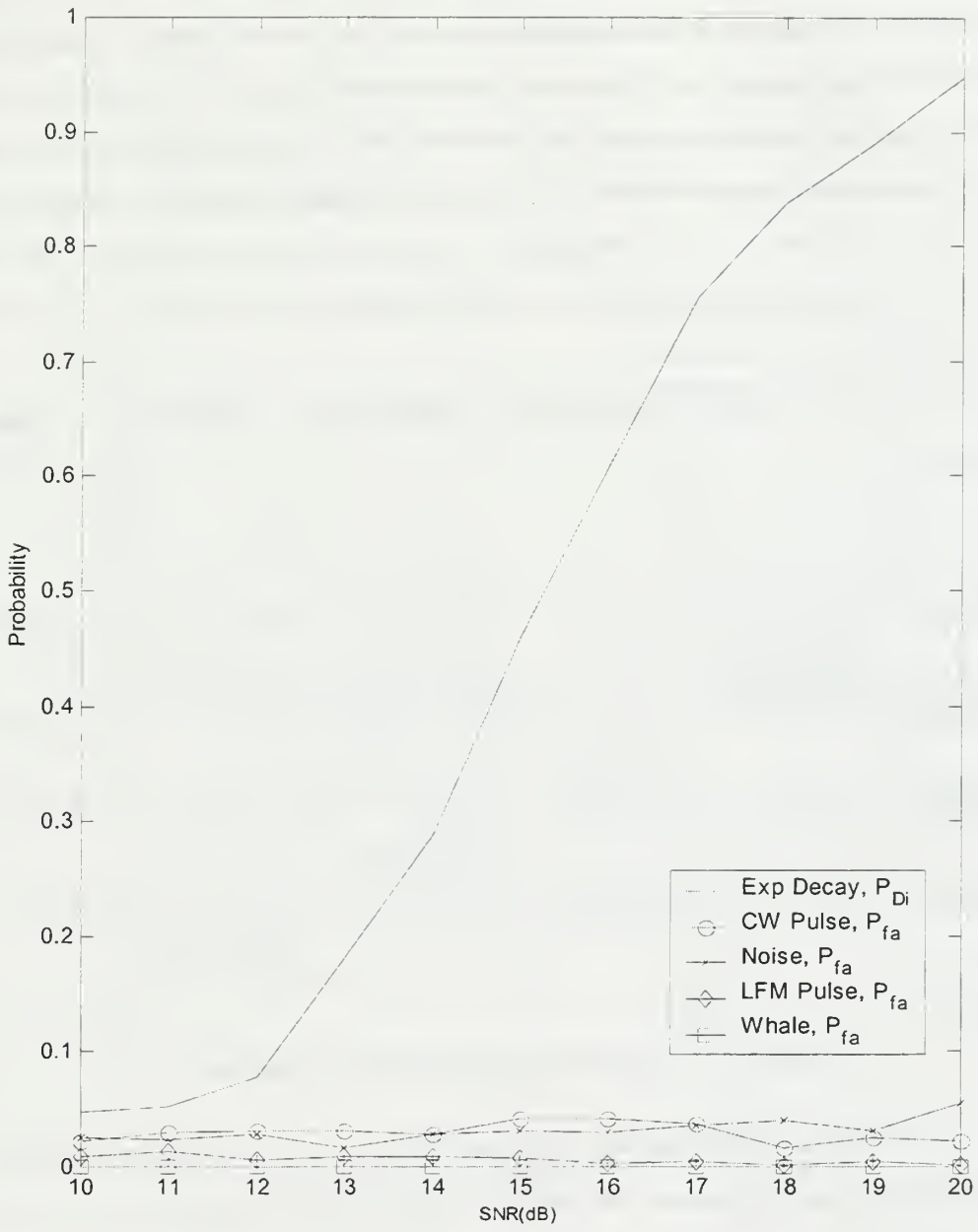


**Figure 22. $P_{Di}$ and $P_{fa}$ (using subspace methods) between exponential decaying transient and exponentially decaying transient, CW Pulse, noise, LFM pulse and whale transient.**

decaying transient arriving at the first and second sonabuoy is shown. It can be seen from this curve that the algorithm discriminates correctly with a $P_{Di}$ of 0.9 or larger for SNR values greater than 17 dB. Figure 22 also shows the $P_{fa}$ for the other transient

arrivals at the second sonabuoy (i.e., CW pulse, LFM pulse, or the whale transient) and the $P_{fa}$ when only noise (no transient) is present at the second sonabuoy. These curves show that the $P_{fa}$ is very low. These are desirable results since they indicate that the algorithm can differentiate between the transients with a high probability of correct discrimination and a low probability of false alarm. Results for the other transients are summarized in Table 4; the corresponding curves are given in appendix A. It is important to note that the results for the whale transient are based on a longer data observation interval than the others.

| Transient Arriving / BUOY 2 / BUOY 1 | CW Pulse | Exponential | LFM Pulse | Whale | Noise |
|---|---|---|---|---|---|
| **CW Pulse** | $P_{Di} \geq 0.35$ for SNR>19dB | $P_{fa} \leq 0.08$ | $P_{fa} \leq 0.01$ | $P_{fa} = 0$ | $P_{fa} \leq 0.01$ |
| **Exponential** | $P_{fa} \leq 0.02$ | $P_{Di} \geq 0.9$ for SNR>17dB | $P_{fa} \leq 0.002$ | $P_{fa} = 0$ | $P_{fa} \leq 0.021$ |
| **LFM Pulse** | $P_{fa} \leq 0.03$ | $P_{fa} \leq 0.08$ | $P_{Di} \geq 0.8$ for SNR>18dB | $P_{fa} \leq 0.1$ | $P_{fa} \leq 0.04$ |
| **Whale** | $P_{fa} \leq 0.2$ | $P_{fa} \leq 0.18$ | $P_{fa} \leq 0.18$ | $P_{Di} \geq 0.8$ for SNR>18dB | $P_{fa} \leq 0.19$ |

**Table 4. $P_{Di}$ results using subspace methods.**

For the bispectral discriminator, the threshold $Q_T$ (see Eq. 3.44) was adjusted by using a threshold gain to improve the results. The gain was applied to Eq. 3.44 in the following way:

$$Q_T = \frac{G}{N-2}\left(\sum_{i=0}^{N-1} \hat{T}(\tau) - Q - Q_2\right) \qquad (5.13)$$

where $G$ is the threshold gain. Threshold gains of 1, 2, 4 and 6 were used.

Figure 23 shows the discrimination results for the exponentially decaying transient using the bispectral discriminator. Again, the vertical axis is labeled "Probability" because both the $P_{fa}$ and $P_{Di}$ are shown on the same plot. For Figure 23, the

transient arriving at sonabuoy 1 is the exponentially decaying sinusoid. The $P_{Di}$ for this transient is shown in Figure 23. The other curves of Figure 23 show the results of the $P_{fa}$ for the CW pulse, noise, LFM pulse and whale transient respectively. The symbols shown in Figure 23 are tied to the transient type and are consistant with what is used in Appendix B. The subplots in Figure 23 show the results when different threshold gains are used.

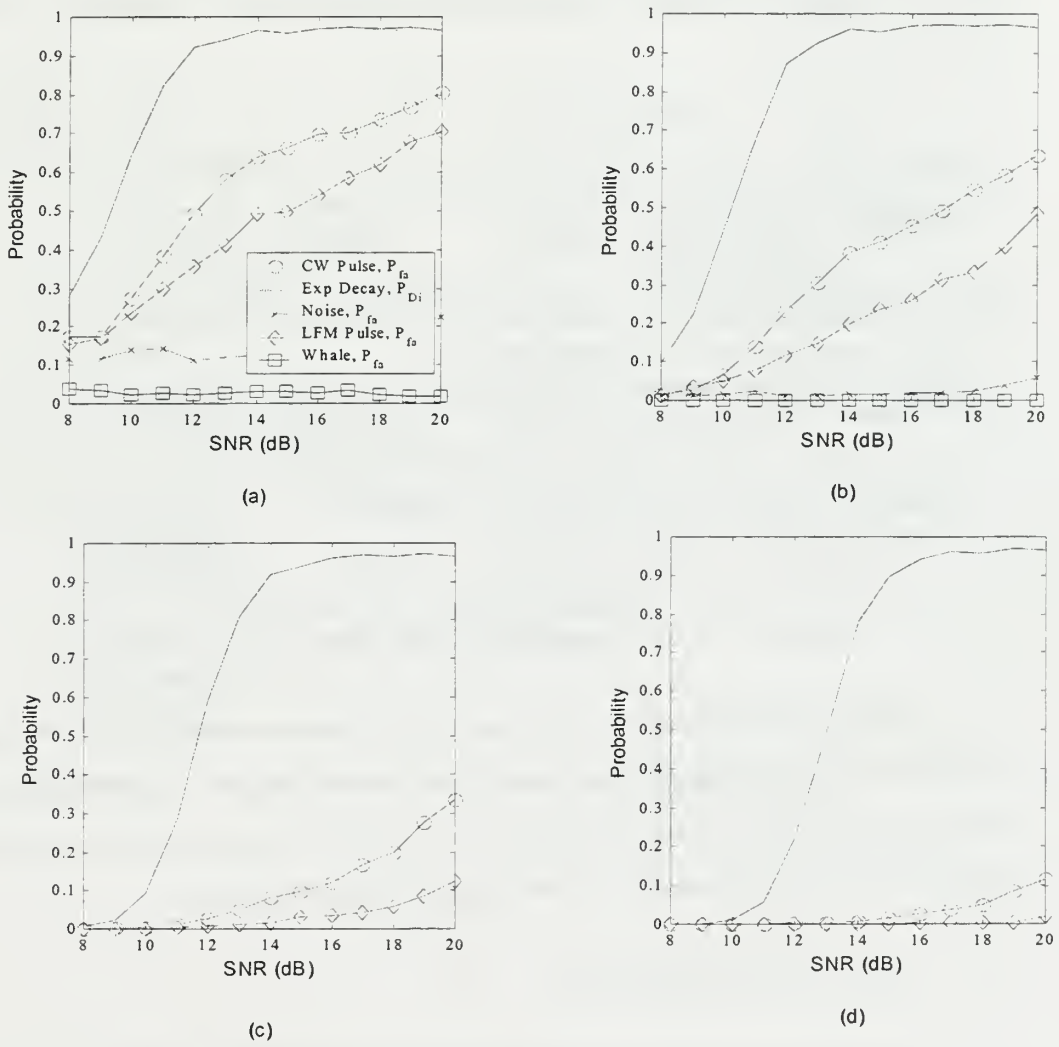


**Figure 23. $P_{Di}$ (using high-order methods) between exponentially decaying sinusoid transient, arriving at sonabuoy 1 and the CW pulse, exponentially decaying Sinusoid, noise, LFM pulse and whale transients arriving at sonabuoy 2. Threshold gain values of (a) 1, (b) 2, (c) 4, (d) 6 were used.**

As can be seen in Figure 23, both $P_{fa}$ and the $P_{Di}$ decrease with increasing threshold gain. A design compromise must therefore be made to have an acceptably high $P_{Di}$ and an acceptably low $P_{fa}$. For this thesis, a threshold gain of 4 was chosen. Table 5 shows the discrimination results for the bispectral discriminator using this value for the threshold gain.

| Transient Arriving / BUOY 2 / BUOY 1 | CW Pulse | Exponential | LFM Pulse | Whale | Noise |
|---|---|---|---|---|---|
| **CW Pulse** | $P_{Di} \geq 0.8$ for SNR $\geq$ 17dB | $P_{fa} \leq 0.2$ | $P_{fa} \leq 0.01$ | $P_{fa} = 0$ | $P_{fa} \leq 0.001$ |
| **Exponential** | $P_{fa} \leq 0.3$ | $P_{Di} \geq 0.98$ for SNR $\geq$ 14dB | $P_{fa} \leq 0.15$ | $P_{fa} = 0$ | $P_{fa} \leq 0.001$ |
| **LFM Pulse** | $P_{fa} \leq 0.05$ | $P_{fa} \leq 0.03$ | $P_{Di} \geq 0.95$ for SNR $\geq$ 16dB | $P_{fa} = 0$ | $P_{fa} \leq 0.001$ |
| **Whale** | $P_{fa} = 0$ | $P_{fa} = 0$ | $P_{fa} = 0$ | $P_{Di} \geq 0.2$ for SNR $\geq$ 20dB | $P_{fa} = 0$ |

**Table 5. $P_{Di}$ using Bispectrum using a threshold gain of 4.**

The poor discrimination performance of the whale transient given in Table 5 may be attributed to the relatively short observation time of the data. Better results may have been obtained if longer observation times were used; however, it was not practical to run a large number of simulations for these longer observation times.

## C. SUMMARY OF RESULTS

The TDOA and discriminator results are summarized in Table 6 including the advantages and disadvantages of both algorithms. As has been previously shown in Figure 18, the bispectral linear phase detector tends to give a larger number of correct TDOA estimates at low SNR. On the other hand, the subspace algorithm gives consistently correct results ($P_T$ = 1.0) at high SNR, which is never achieved by the

bispectrum algorithm for SNR in the range of 8 dB to 20 dB. Therefore the more desirable result may depend on the application where the algorithms will be used.

For discrimination, the bispectral method gave the highest $P_{Di}$ results when a threshold gain of 4 was used. However, the $P_{fa}$ increased with increasing SNR (see Figure 23). This is an undesirable result since even transients with high SNR will not be able to be separated. On the other hand, the subspace discriminator gave lower $P_{Di}$ values but had the advantage that the $P_{fa}$ remained constant for all SNR values tested.

| **Algorithm** | **TDOA** | **Discrimination** |
|---|---|---|
| Bispectrum | **Best Result:** SNR > 11dB gives a $P_T$ of 0.9 (exponential transient)<br>**Disadvantage**: A $P_T$ of 1 is never achieved at SNRs < 20dB<br>**Advantage**: High $P_T$'s are achieved at low SNRs | **Best Result**: SNR > 14dB gives a $P_{Di}$ of 0.98 (exponential transient).<br>**Disadvantages**: Results depend on choice of threshold gain. $P_{fa}$ increases with increasing SNR.<br>**Advantages**: Can achieve a high $P_{Di}$ at relatively low SNRs. Has a low $P_{fa}$ for noise |
| Subspace | **Best Result:** SNR > 17dB gives a $P_T$ of 1. (exponential transient)<br>**Disadvantage**: High $P_T$'s are only achieved at high SNRs<br>**Advantage**: $P_T$'s of 1 are achieved. | **Best Result**: SNR > 17dB gives a $P_{Di}$ of 0.9 (exponential transient).<br>**Disadvantages**: Computationally intensive. Low $P_{Di}$ at high SNRs<br>**Advantages**: Low $P_{fa}$ for all transients |

**Table 6. Summary of TDOA and discrimination results.**

THIS PAGE INTENTIONALLY LEFT BLANK

# VI. CONCLUSIONS

## A. THESIS SUMMARY

In this thesis, we have developed and compared two algorithms, namely the bispectrum and subspace linear phase detectors. These algorithms were developed for the purposes of transient discrimination and TDOA estimation, in order to be used as part of a transient tool suite to aid in the estimation of a submarine's position. Chapters III and IV of this thesis provide an analysis of these two algorithms. Two performance measures were used to evaluate the algorithms, namely the probability of correct TDOA ($P_{T)}$ and the probability of correct discrimination ($P_{Di}$).

Chapter V discusses the simulations and transients used in the evaluation of the algorithms. Of the four transients used, it was found that the whale transient, which is the longest transient, gave the worst performance. This may be due to the relatively short data observation times used in evaluating the algorithms. It was found that longer observation times produced better results for this transient; however, it was impractical to run a large number of cases at the longer observation times.

It was found that both algorithms had advantages and disadvantages as summarized in Table 6. In general, it can be said that for TDOA the bispectral linear phase detector gave better results at low SNR while the subspace linear phase detector worked better at the higher SNR.

For discrimination, it was found that the bispectral discriminator gave higher $P_{Di}$ than the subspace discriminator. However, the $P_{fa}$ of the bispectral discriminator increased at higher SNR while the subspace discriminator gave a constant $P_{fa}$ for all SNR values tested. For discrimination, the advantage of having a constant $P_{fa}$ is desirable. Therefore the subspace discriminator is the best option even although it produced lower $P_{Di}$ than the bispectral discriminator. As discussed in Chapter V, there are design trade offs between processing speed and performance that need to be made. For the bispectral linear phase detector, this trade off is in terms of threshold gain; for the subspace linear phase detector, this trade off is in terms of correlation matrix size.

## B. FUTURE WORK

The results of this thesis lead to some interesting topics for future research. These topics include:

(1) **The effects of the environment on a transient**. In the evaluation of the two algorithms conducted in this thesis, no work was done to determine the sensitivity of the algorithms to changes in transient shape due to the environment. To do this, a propagation model must be used.

(2) **The effects of colored noise**. In the simulations additive white Gaussian noise was used. This is a poor reflection of reality since ocean noise is frequently colored [Ref 22]. It will therefore be important to see how these algorithms perform when additive colored noise is used.

(3) **Operational testing**. The algorithms were tested using synthetic data. Ultimately, there is a need to test them on real data to obtain a measure of their performance and applicability in the field.

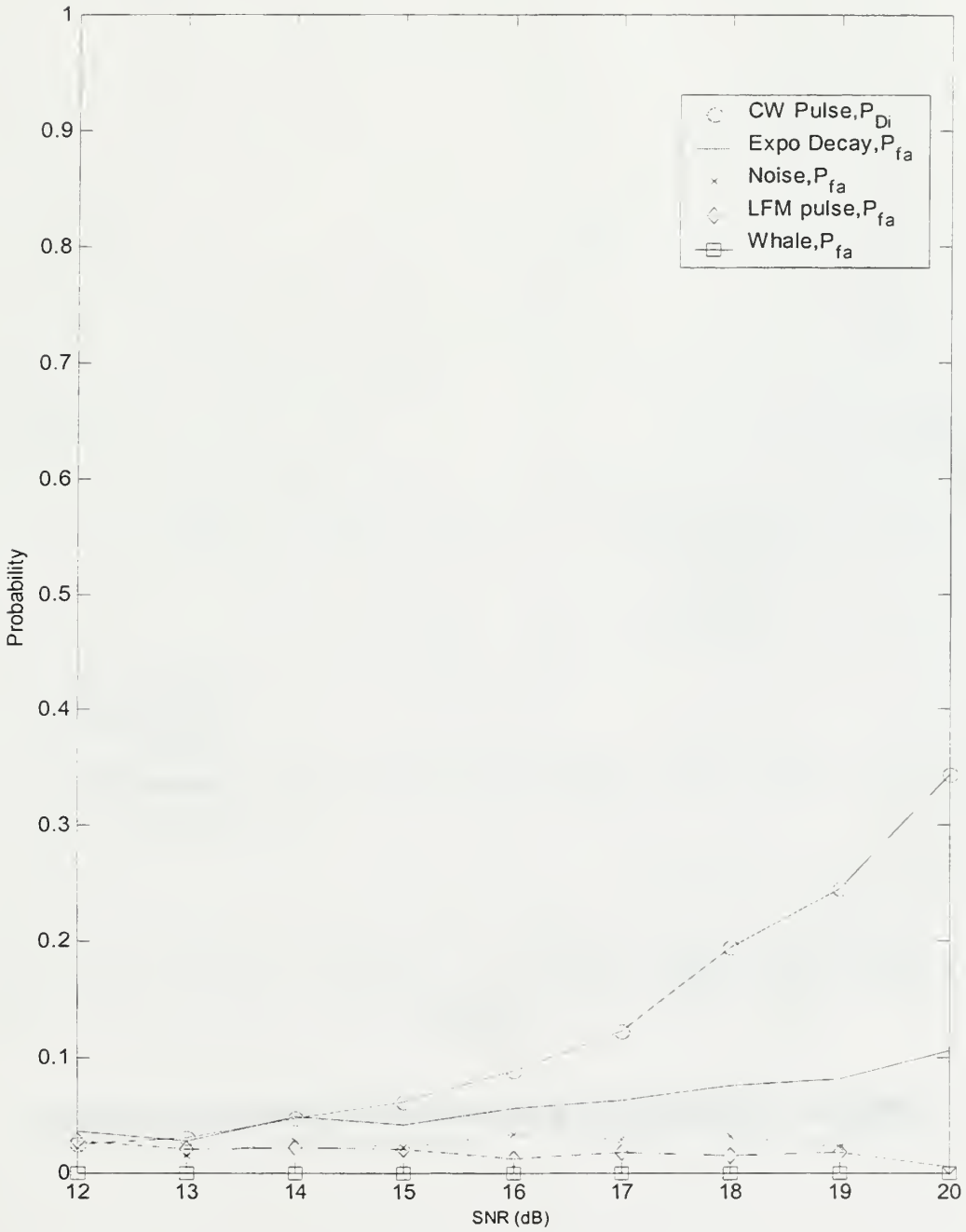


**Figure 24. $P_{Di}$ for the CW transient arriving at the first sonabuoy.**

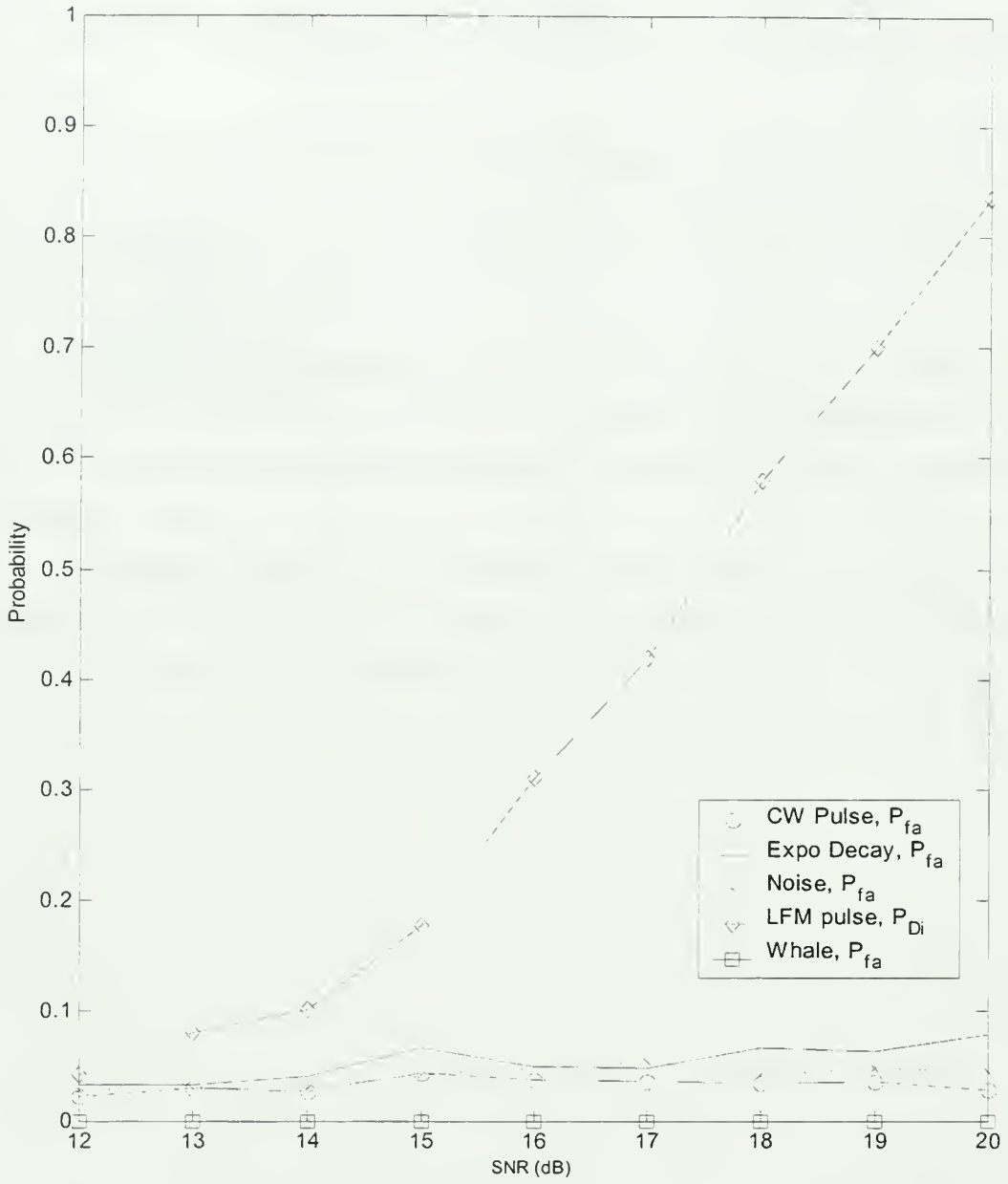


**Figure 25. $P_{Di}$ for the LFM transient arriving at the first sonabuoy.**

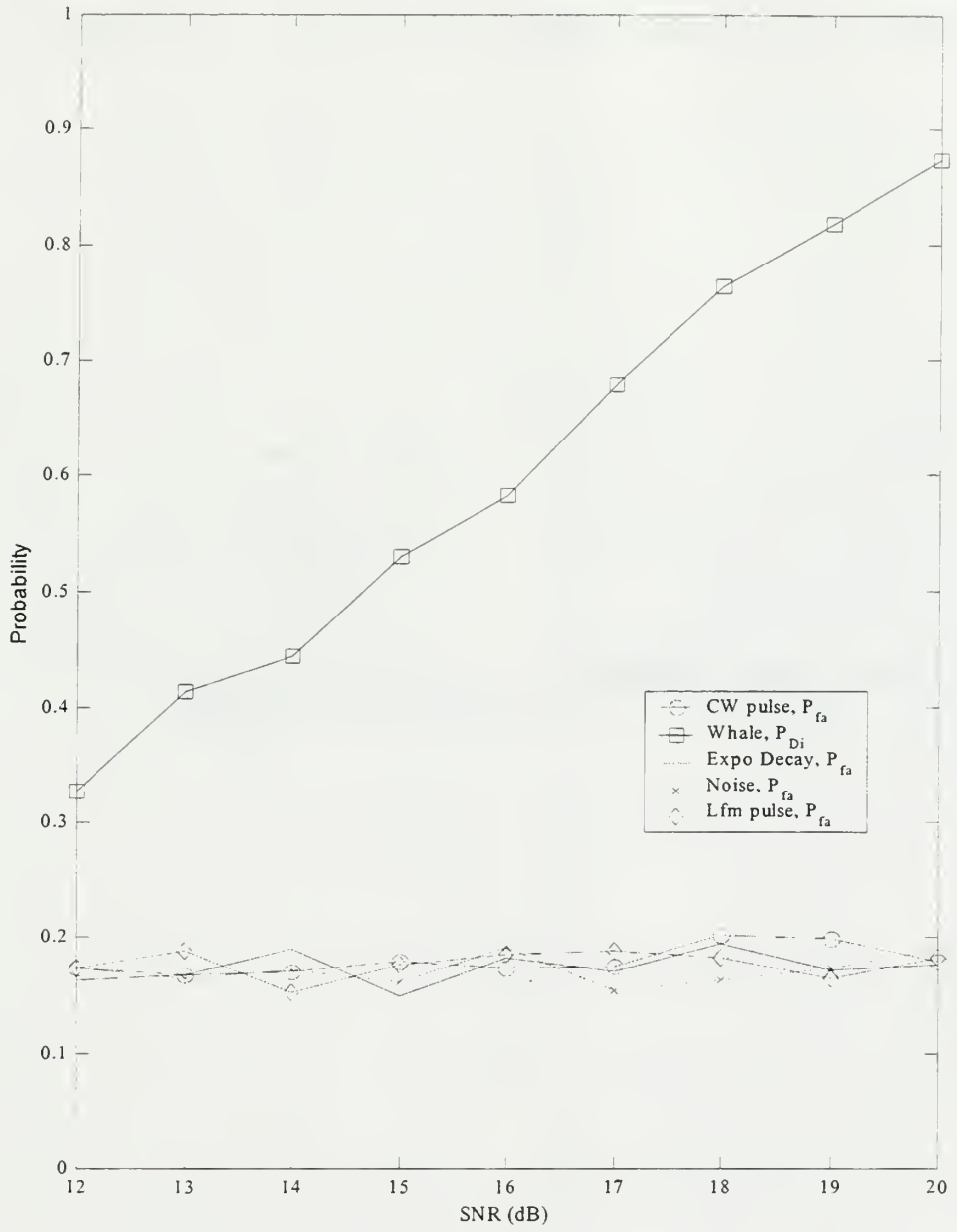


**Figure 26. $P_{Di}$ for the whale transient arriving at the first sonabuoy.**

THIS PAGE INTENTIONALLY LEFT BLANK

## APPENDIX B $P_{DI}$ AND $P_{FA}$ USING BISPECTRUM METHOD

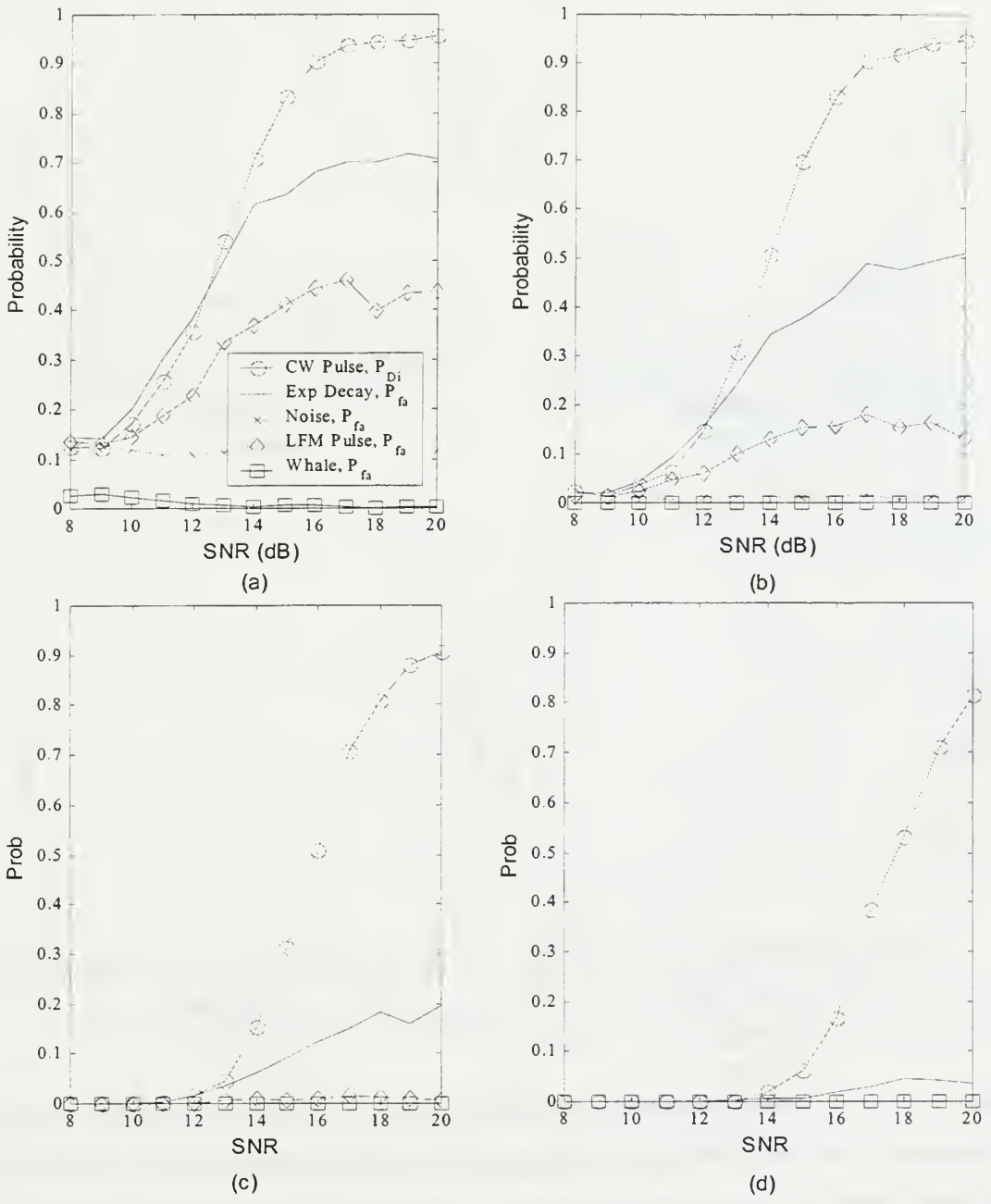


**Figure 27. $P_{Di}$ (using bispectral methods) between CW pulse transient , arriving at sonabuoy 1 and the CW pulse, exponentially decaying sinusoid, noise, LFM pulse and whale transients arriving at sonabuoy 2. Threshold gain values of (a) 1, (b) 2, (c) 4, (d) 6 were used.**

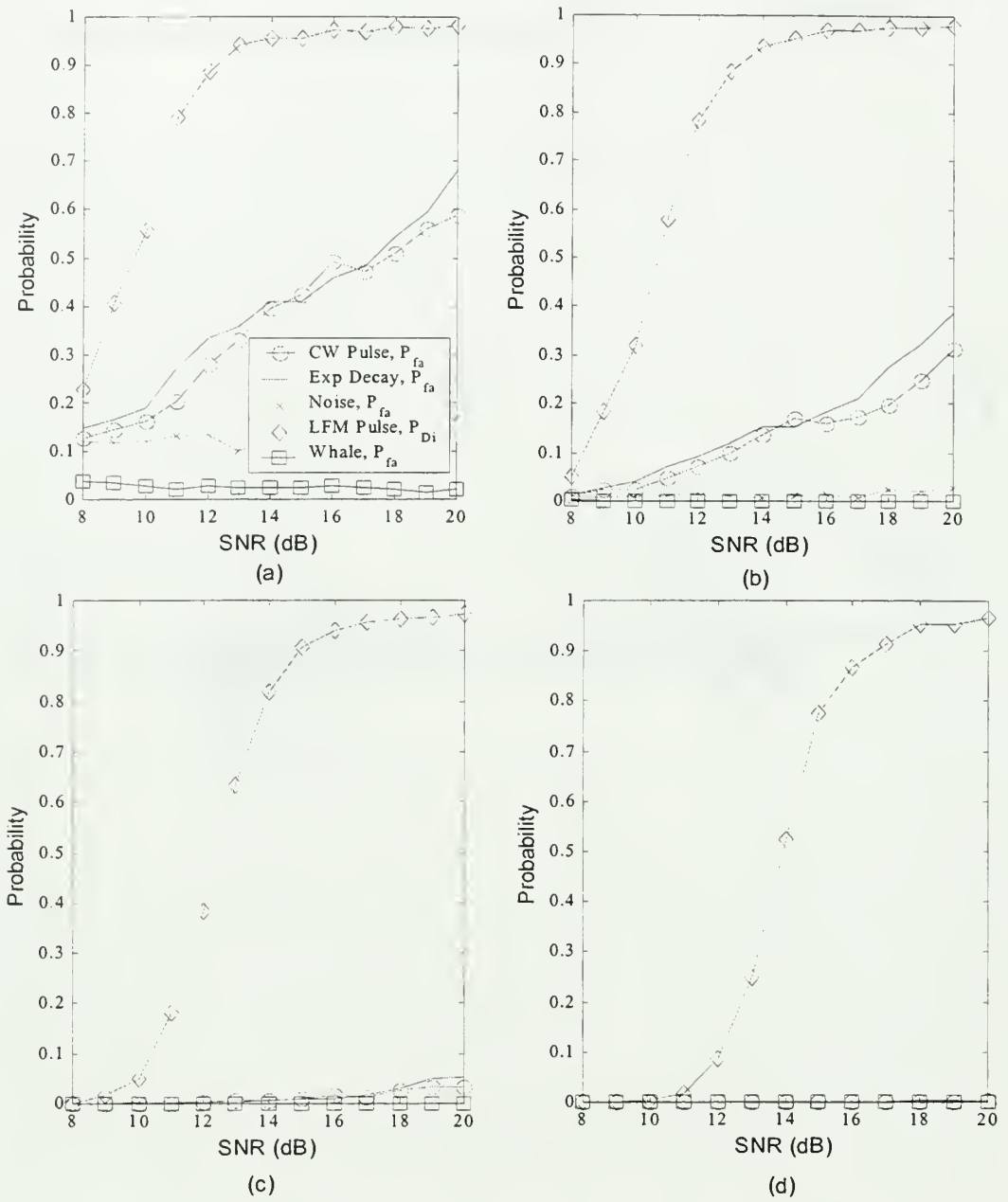


**Figure 28. $P_{Di}$ (using bispectral methods) between LFM pulse transient , arriving at sonabuoy 1 and the CW pulse, exponentially decaying sinusoid, noise, LFM pulse and whale transients arriving at sonabuoy 2. Threshold gain values of (a) 1, (b) 2, (c) 4, (d) 6 were used.**

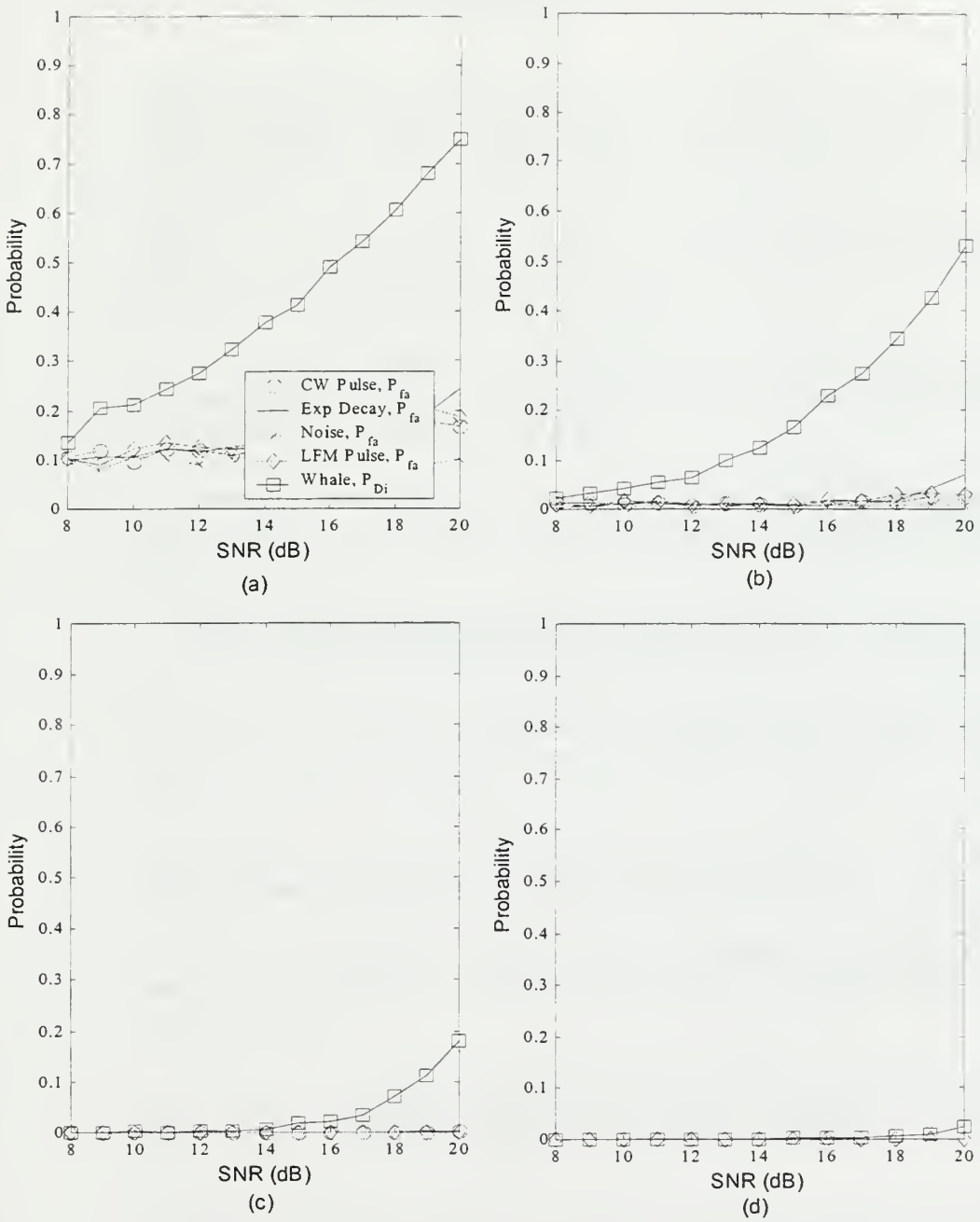


**Figure 29. $P_{Di}$ (using bispectral methods) between whale transient , arriving at sonabuoy 1 and the CW pulse, exponentially decaying sinusoid, noise, LFM pulse and whale transients arriving at sonabuoy 2. Threshold gain values of (a) 1, (b) 2, (c) 4, (d) 6 were used.**

THIS PAGE INTENTIONALLY LEFT BLANK

## LIST OF REFERENCES


[1] Rafael Widow, "Development of Visual C++ Version of the Braodband Cross-Correlation Time Delay Tracker Module for S2K," Naval Postgraduate School, Monterey, CA, Master's. Thesis, September 1999.

[2] Knapp. C. H. and G. Carter, "The Generalised Correlation Method for Estimation of Time Delay," *IEEE Trans. Acoustics, Speech and Signal Processing*, ASSP-36, pp 757-763, Aug. 1976.

[3] M. Wax, "The Estimate of Time Delay Between Two Signals with Random Relative Phase," *IEEE Trans. Acoustics, Speech and Signal Processing*, 29(3), pp 497-501, June 1981.

[4] E. Hannan, "Delay Estimation and the Estimation of Coherence and Phase," *IEEE Trans. Acoustics, Speech and Signal Processing*, 29(3), pp 485-489, June 1981.

[5] A. Piersol, "Time Delay Estimation Using Phase Data," *IEEE Trans. Acoustics, Speech and Signal Processing*, 29(3), pp 471-477, June 1981.

[6] B. Porat *et al*, "Adaptive Detection of Transient Signals," *IEEE Trans. Acoustics, Speech and Signal Processing*, 34(6), pp 1410-1418, Dec. 1986.

[7] Chrysostomos L. Nikias, Athina P. Petropulu, *Higher-Order Spectral Analysis*, Prentice Hall, Engelwood Cliffs, New Jersey, 1993.

[8] Lisa Pflug, "Properties of Higher Order Correlations and Spectra for Bandlimited, Deterministic Signals," *Journal Acoust. Soc Am.* 91(2), Feb 1992, pp 975-988.

[9] Lisa Pflug *et al*, "Prediction of Signal-to-Noise Ratio Gain for Passive Higher-Order Correlation Detection of Energy Transients," *Journal Acoust. Soc Am.* 98(1), July 1995, pp 248-259.

[10] M. Hinich, "Detecting a Transient Signal by Bispectral Analysis," *Journal Acoust. Soc Am.*38(7), July 1990, pp 1277-1283

[11] Lisa Pflug, *et al*, "Detection of Oscillatory and Impulsive Transients Using Higher-Order Correlations and Spectra," *Journal Acoust. Soc Am.* 91(5), May 1992.

[12] M. Bartlett *et al*, "Transient detection using the nonstationary bispectrum," *Journal Acoust. Soc Am.*99(5), May 1996, pp 1277-1283.

[13] P. R. Roth, "Effective Measurements Using Digital Signal Analysis," *IEEE Spectrum* vol8, pp 62-70, Apr. 1971.

[14] G. C. Carter, A. H. Nuthall and P. G. Cable, "The Smoothed Coherence Transform," *Proc. IEEE* 61(10) , pp 1494-1498, Oct. 1973.

[15] G. C. Carter, A. H. Nuthall and P. G. Cable, "The Smoothed Coherence Transform," Naval Underwater System Center, New London Lab, New London, CT, Tech. Memo 2020-34-6, Feb. 27, 1969.

[16] Nikias, C. L and R. Pan, "Time Delay Estimation in Unknown Gaussian Spatially Correlated Noise," *IEEE Trans. Acoustics, Speech and Signal Processing*, 36(11), pp 1706-1714, November 1988.

[17] Charles W. Therrien, *Discrete Random Signals and Statistical Signal Processing*, Prentice Hall, Prentice Hall, Engelwood Cliffs, New Jersey, 1992.

[18] Ralph Schmidt, "Multiple Emitter Location and Signal Parameter Estimation," *IEEE Trans. Antennas and Propagation*, AP-34:276-290, March 1986.

[19] F. G. Stremmeler, *Introduction to Communication Systems*, 2nd., Addison-Wesley, Menlo Park, CA,1982.

[20] C. W. Therrien, S. D. Kouteas, K. B. Smith, "Time Delay Estimation Using a Signal Subspace Model", *Proc. Asilomar Conf. on Signals*, Systems and Computers, November 2000.

[21] S. D. Kouteas, "Time Delay Estimation for Underwater Signals and Application to Localization," Naval Postgraduate School, Monterey, CA, Master's. Thesis, (in progress).

[22] K. Frack, "Improving Transient Signal Synthesis Through noise Modeling and Noise Removal," Naval Postgraduate School, Monterey, CA, Master's. Thesis, March 1994.

## INITIAL DISTRIBUTION LIST

1. Defense Technical Information Center ..... 2
   8725 John J. Kingman Rd., STE 0944
   Ft. Belvoir, Virginia 22060-6218

2. Dudley Knox Library ..... 2
   Naval Postgraduate School
   411 Dyer Rd.
   Monterey, CA 94943-5101

3. Professor Murali Tummala, Code EC/Tu ..... 1
   Department of Electrical and Computer Engineering
   Naval Postgraduate School
   Monterey, CA 93943-5121

4. Professor Charles Therrien, Code EC/Ti ..... 1
   Department of Electrical and Computer Engineering
   Naval Postgraduate School
   Monterey, CA 93943-5121

5. Professor Jeffrey Knorr, Code EC/Ko ..... 1
   Department of Electrical and Computer Engineering
   Naval Postgraduate School
   Monterey, CA 93943-5121

6. Professor Kevin Smith, Code PH/Sk ..... 1
   Physics Department
   Naval Postgraduate School
   Monterey, CA 93943-5717

7. Dr. Michael Shields, Code EC/Si ..... 1
   Department of Electrical and Computer Engineering
   Naval Postgraduate School
   Monterey, CA 93943-5121

8. CAPT L. V. Judge ..... 1
   PEO(A) Air ASW, Assault and Special Mission Programs PMA-264
   47123 Buse RD IPT Ste 148
   Patuxent River, MD 20670-1547

9. LCDR Ron Higgs ..... 1
   PEO(A) Air ASW, Systems Program Office PMA-264D2
   APM for Non-acoustic ASW
   47123 Buse RD IPT Ste 148
   Patuxent River, MD 20670-1547

10. Mike Worthington ..... 1
Maritime Surveillance Associates
PO Box 90475
Portland, OR 97290-0475

11. CNavy ..... 1
Navy Office
Private Bag X104
Pretoria, South Africa 0001

12. LCDR Granger Bennett ..... 1
5 Tobago Way
Capri Village, South Africa 7975